Inhomogeneities and Cell-to-Cell Variations in Lithium-Ion Batteries, a Review

David Beck [1,†] , Philipp Dechent [2,3,†] , Mark Junker [2,3], Dirk Uwe Sauer [2,3,4] and Matthieu Dubarry [1,*]

1   Hawaii Natural Energy Institute, University of Hawaii at Manoa, 1680 East West Road, POST109, Honolulu, HI 96815, USA; dmbeck@hawaii.edu
2   Institute for Power Electronics and Electrical Drives (ISEA), RWTH Aachen University, 52066 Aachen, Germany; Philipp.Dechent@isea.rwth-aachen.de (P.D.); Mark.Junker@isea.rwth-aachen.de (M.J.); sr@isea.rwth-aachen.de (D.U.S.)
3   Juelich Aachen Research Alliance, JARA-Energy, 52062 Aachen, Germany
4   Forschungszentrum Juelich GmbH, IEK-12, Helmholtz-Institut Münster, co ISEA of RWTH Aachen University, 52066 Aachen, Germany
*   Correspondence: matthieu@hawaii.edu
†   These authors contributed equally to this work.

Abstract: Battery degradation is a fundamental concern in battery research, with the biggest challenge being to maintain performance and safety upon usage. From the microstructure of the materials to the design of the cell connectors in modules and their assembly in packs, it is impossible to achieve perfect reproducibility. Small manufacturing or environmental variations will compound big repercussions on pack performance and reliability. This review covers the origins of cell-to-cell variations and inhomogeneities on a multiscale level, their impact on electrochemical performance, as well as their characterization and tracking methods, ranging from the use of large-scale equipment to in operando studies.

1. Introduction

With sustainability being the new paradigm for development, today's world is relying more and more on clean energy storage technologies to help meet and keep up with the ever-demanding energy goals. Thanks to their high power and energy densities, good cycle life and excellent storage capabilities, Li-ion batteries are the product of choice and are currently dominating the field of electrochemical energy storage. The biggest challenge in using Li-ion batteries is to maintain performance and safety upon usage; this ideally requires keeping all the cells balanced and homogeneously degraded. This is complex as most applications require large battery packs comprising hundred to thousands of cells that do not necessarily come from the same production batches nor are going to experience the same currents or temperatures.

Different approaches are possible when assembling battery packs with different pro and cons on inhomogeneities and cell-to-cell variations (ctcV). Some assemblers are choosing to use cylindrical cells that are manufactured by the million with tightly controlled characteristics, with the drawback of complicating assembly and control. Others are choosing to use larger pouch or prismatic cells to limit the number of cells within a battery pack. This eases assembly and control, but larger cells are usually more expensive and manufactured in much smaller numbers which could make them more susceptible to ctcV. In addition, because of the size of the battery packs and the size of the electrodes in each single cell, electrodes often face inhomogeneous conditions upon aging, independently of the form factor of cells used.

Although ctcV and inhomogeneities plays a key role on the performance and durability of large batteries, no review solely focused on their origin and their characterization is, to the best of our knowledge, available. These topics were partially addressed in [1] for ctcV, Reference [2] for material design, Reference [3] for electrode processing, and [4–9] for characterizations, invasive or not, but not comprehensively. To fill this gap, this review summarizes the state-of-the-art of understanding and characterization of ctcV and inhomogeneities observed upon aging. They were tackled with a bottom-up approach from materials to battery packs and ending on the proposed characterizations.

2. Origins of Cell-to-Cell Variations (ctcV) and Inhomogeneities

From the fabrication of electrodes to the assembly in cells then packs, it is impossible to achieve 100% consistency with a zero-fault design and this will lead to intra- and inter- cell variations, Figure 1. During material synthesis micro tolerances or variations, among others, could lead to differences in structure, composition, or morphology [10]. Internal non-uniformities, such as disparities in architecture, composition or calendering, might affect the initial performance of electrodes of which assembly and winding can also induce inhomogeneous degradation [11,12]. At the pack or module level, variations in wiring resistance, welding process, connectors, and environmental factors also influence the overall performance and degradation [13,14] by affecting local state of health, temperature, or current distribution. This first section presents a description and assessment of root causes, mechanisms and effects of inhomogeneities scaling from the materials to the electrodes, then to the cell level, and battery packs. For ease of discussion, intra-cell variations will be referred to as inhomogeneities and inter-cell variations as ctcV.
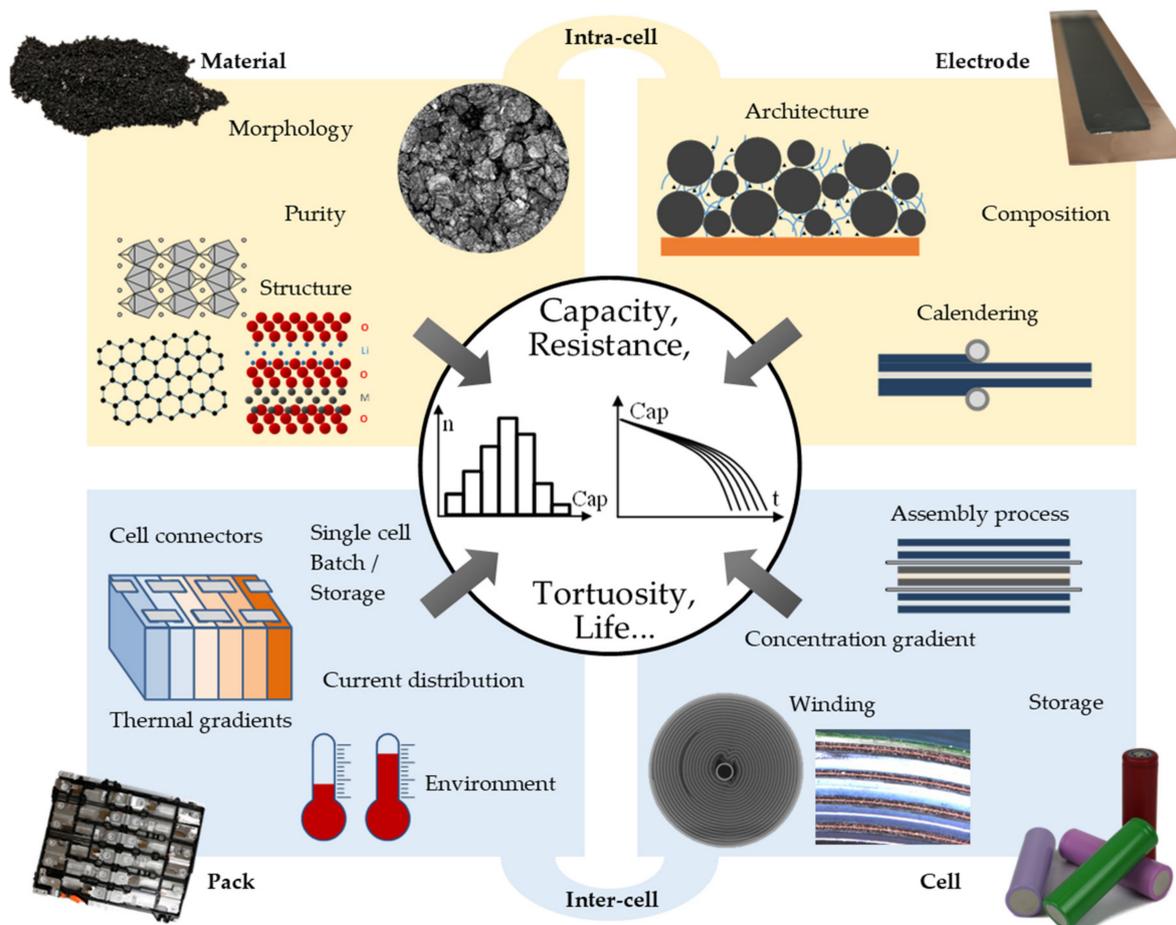

Figure 1. Multiscale breakdown of the origins of intra (yellow) and inter-cell (blue) variations.

2.1. Material and Electrode Levels

2.1.1. Microstructure and Composition

The electrode composition, microstructure, and architecture play a key role in shaping cell performance. Battery electrodes are complex and require active materials for capacity, additives for electronic conductivity, binder to maintain mechanical integrity, and porosity to allow ionic conductivity. Transport parameters such as ion diffusion, as well as ionic and electric conductivity highly depend on the different pathways through the electrodes [15–18]. Any defects or irregularities in the electrode materials can cause local inhomogeneities that will directly affect the performance, durability and safety.

The first critical source of these local inhomogeneities stems from the base materials themselves. Manufactured electrodes will be affected by the characteristics and the quality of the precursor materials. This includes, among others, inhomogeneities in composition, purity, defects, and morphology. Several authors have indirectly investigated the impact of these inhomogeneities on cell performance. Harris et al. [11] showed that the structure of the graphite electrode from a commercial laptop battery was non-uniform comprising of high and low tortuosity subregions. Low tortuosity regions were suspected to be subjected to higher Li^+ ions concentration which could increase local current density and lead to local overcharging [19]. This could in turn cause structural disordering or cracking of the electrode and lithium plating [20,21] but also lead to temperature gradients. Vice versa, high tortuosity regions could deter Li^+ ions and cause some areas to be left delithiated, lowering the capacity of the battery [22,23]. Müller et al. [24] found microstructural inhomogeneities between graphite electrodes from different manufacturers at different length scales, Figure 2. Differences in grain size (Figure 2a) lead to different porosity (Figure 2b) and tortuosity (Figure 2c) values between electrodes. In addition, within an electrode, tortuosity also appeared to be anisotropic (Figure 2c) with higher values in the direction perpendicular to the current collector (TP on Figure 2c). Samples taken millimeters apart were shown to have different overpotentials during lithiation which can cause the potential of the electrode to drop below 0 V vs. Li^0/Li^+, triggering lithium plating.
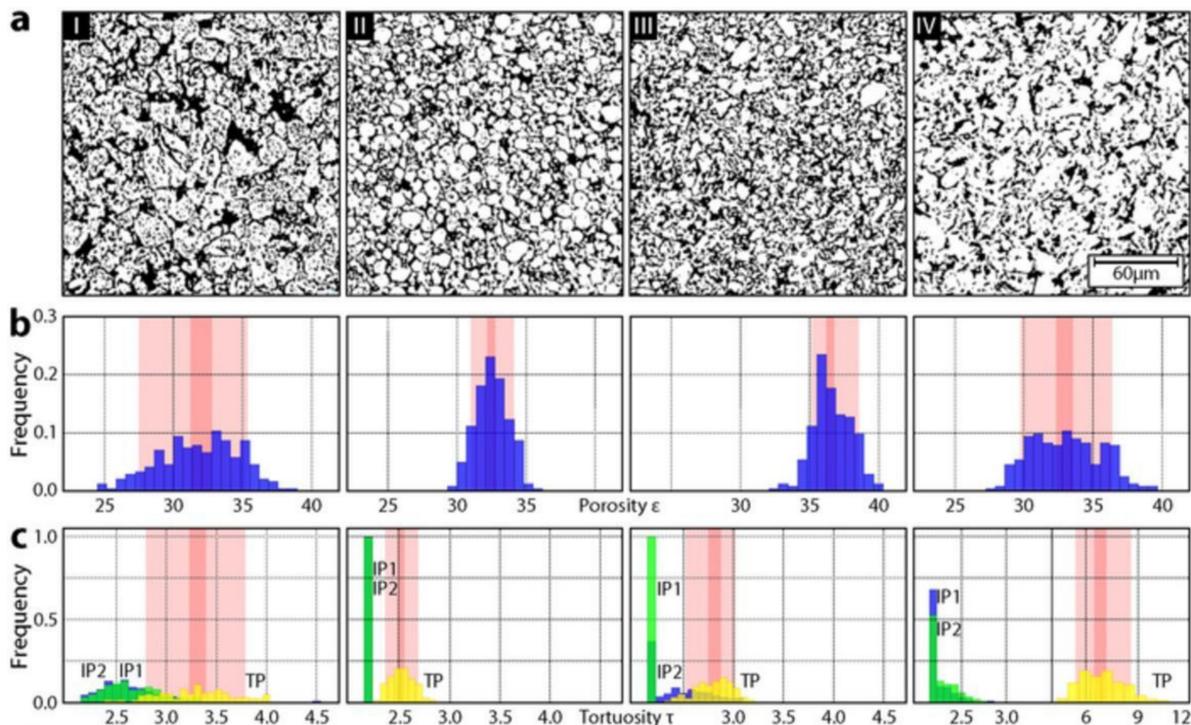

Figure 2. Tomogram results of one sample of four different negative electrodes revealing: (**a**) the types of graphite particles with associated (**b**) porosity and (**c**) tortuosity. IP1 and IP2 correspond to two in-plane directions while TP corresponds to the through-plane direction (modified from CC BY Müller et al. [24]).

Dubarry et al. [25] and Pavoni et al. [26] showed that grain size distribution can also drastically affect the kinetics of the electrochemical response. Yang et al.'s [27] in situ optical observations revealed gas and/or electrolyte filled defects in the electrodes that affected Li^+ ion diffusion. Gas-filled defects decelerate Li^+ ions while electrolyte-filled defects accelerate them. This phenomenon also contributes to uneven Li^+ ion distribution. Liu et al. [28] proposed to predict the occurrence of lithium plating by analyzing the shape and size of localized inhomogeneities. Results show that, for equal surfaces, areas with larger inhomogeneities were more degraded than areas with clusters of smaller inhomogeneities. Pouraghajan et al. [29] found a strong dependance between ionic/electronic conductivities and cell chemistry. Differences in specific areas will also affect Li^+ ion transport and can lead to inhomogeneous distributions of current then eventually to the failure of the cell [28,30,31].

During cycling, microcracks can also occur in the active material because of the volumetric changes associated with Li^+ intercalation. Concentration gradients within grains leading to localized volumetric changes are believed to be the fundamental root cause of the microcracking as well as the fracturing, and cracking of electrodes [32,33]. This will affect electrode tortuosity and electronic resistivity. Microcracks were shown to happen on graphite [34,35], silicon [36–38], and some positive electrode (PE) materials [33,39,40]. Several studies observed increased polarization and poorer electrical contact between active particles and the current collector. However, this electrochemical milling does not always result in worsening performances as it could increase the amount of accessible intercalation sites, decreasing electrode tortuosity by opening pores and creating new ionic pathways. Birkl et al. [41] showed that graphite electrodes in a Graphite//$LiCoO_2$ (LCO)–$NiMnCoO_2$ (NMC) pouch cells that were non-uniformly lithiated exhibited a higher capacity than the homogeneous cell. Dubarry et al. [42] found that electrode cracking could improve kinetics of an LFP electrode by increasing the specific surface area of the grains.

2.1.2. Electrode Fabrication

Beyond the materials, proper fabrication of electrodes is also essential to obtain a consistent architecture. As shown in Figure 3, the manufacturing process of lithium-ion battery electrodes involves many steps such as the weighing of active materials, the application of the slurry on the current collectors, and the calendering process to smoothen and flatten the electrodes [43]. These steps must be done with precision to achieve consistent porosity and tortuosity. Improper mixing of the electrode slurry can lead to the inhomogeneous distribution of the active materials and additives. When coating the electrodes after the desired formulation is obtained, Higa et al. [44] reported that active material was found to be more uniformly distributed on the electrode when slurry viscosity and heating power were higher. In [45], Lenze et al. described the impact of deliberate variations within manufacturing parameters on the performance of lithium-ion batteries. Four sets of cathode recipes, each with different active mass loading and calendering settings were prepared. The evaluation of the resulting energy and power density show influence in order of magnitudes and high sensitivity. With similar results, Dreger et al. [46] compared different dispersing procedures and their impact on performance. Kenney et al. [47] set out to link the impact of variations in the electrode manufacturing process (electrode thickness, electrode density and active material) to the capacity of lithium-ion battery modules. Recent optimization work from Rynne et al. [48] showed the potential for design of experiments (DOE) in electrode formulation. The group studied almost 100 different electrode formulations and was the first to openly report empirical equations linking electrode microstructure to cell behavior. Results indicate that higher cell performance is linked to high active material content with a small fraction of conductive additives as well as minimal binder content.
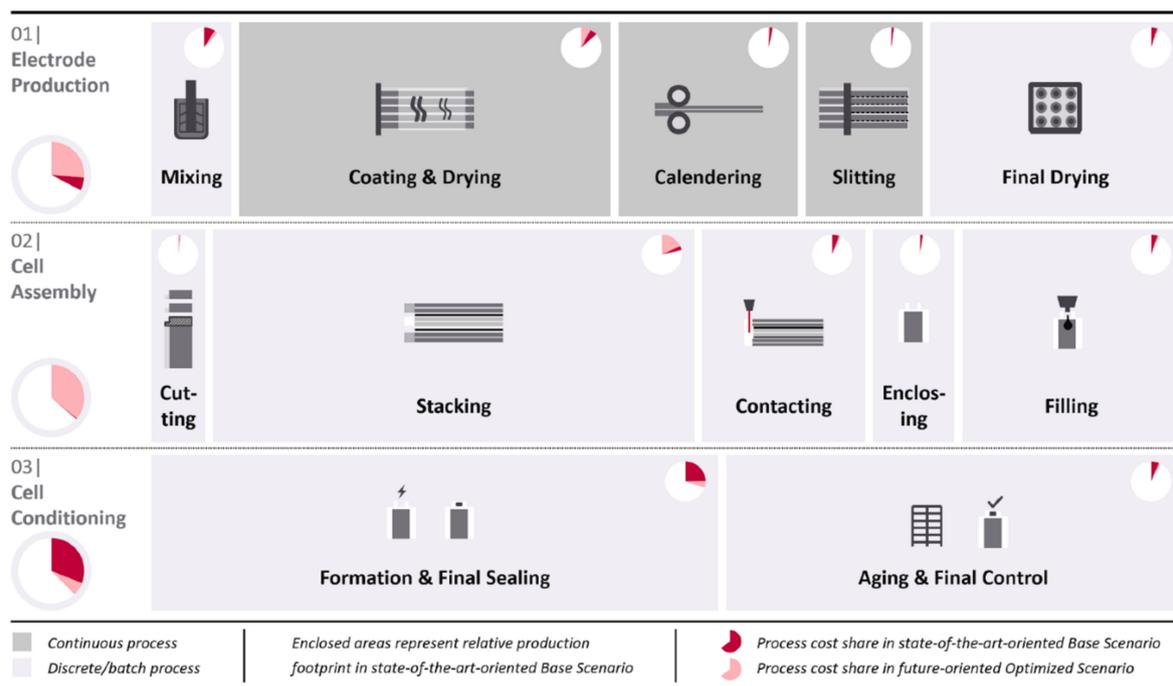
Figure 3. Manufacturing process steps of a lithium-ion pouch cells (CC BY Mauler et al. [49]).

The influence of the calendering process on the pore size distribution and particle deformation was investigated by several groups like Haselrieder et al. [50], Ngandjong et al. [51] and Kang et al. [52]. Schmidt et al. [53] studied highly compressed NMC electrodes and found optimum calendering/compression rates necessary to obtain high-capacity retention while being able to deliver good power and long-term performance. Production parameters, therefore, must be tightly controlled to ensure consistent quality.

Although a lot of work has been done in material synthesis and processing, further engineering and optimization [48] of the electrode microstructure, especially with the help of modeling [54–56] and of new machine learning techniques [57], is vital to achieve high homogeneity and high transport parameters in order to minimize the effects of inevitable manufacturing tolerances—whether it be large scale or laboratory scale manufacturing—on the development of high-performance cells.

2.2. Cell Level

2.2.1. Intrinsic

A typical commercial cell is far more complex than the simple schematic of a battery with two electrodes separated by a separator. During cell assembly, process-related inaccuracies can also cause the cells to behave inhomogeneously [58]. These homogeneities will also be influenced by the construction of the cells—cylindrical, prismatic or pouch—because of the variations in production process between the different formats. For the classic cylindrical 18,650 cells, once the electrodes have been sized accordingly, the components are assembled into a separator-negative electrode-separator-positive electrode stack then wound into a jelly roll. The jelly rolls are then inserted in cylindrical cases, and conducting tabs are welded on the terminals. Prismatic cells generally consist of long stacks of electrodes similar to those of cylindrical cells but folded and pressed to fit into a hard rectangular casing instead of being wound. Pouch cells do not have a rigid enclosure and use stacked paralleled electrodes without winding or folding. The negative (NE) and positive (PE) electrodes are cut into individual rectangles which are stacked alternately and separated by the separator, then sealed in an aluminum pouch. The assembly process of a lithium-ion battery is very intricate [49] and Figure 3 highlights the high number of necessary steps for a pouch cell.

Tight measures must be put in place to ensure minimal variations. Leithoff et al. [58] studied the effect of electrode deposition accuracy during the stacking process and found a linear relationship between the nonoverlapping of the electrodes and discharge capacity. Paxton et al.'s [59] results reveal asynchronous discharge behavior and incomplete electrode utilization. Ziesche et al. [60] noticed that pristine cells already showed cracks on the PE, most definitely after-effects of the production process. The cracking is accentuated when moving towards the center of the cell where the electrode's bending radius is higher.

Small variations are impossible to avoid and cells from the same production line are usually sold in different grades to account for intra-batch inhomogeneities. Ranging from smaller scale testing [61–65] to larger scale testing [10,65–71], many studies reported cell-to-cell variations within batches. Dubarry et al. [69] were among the first to conduct systematic campaigns of ctcV characterization on new batches of cell and characterized them with three independent attributes: the amount of active material, the polarization resistance, and the rate capability. In [70], they also investigated variations in the electrode loading ratio and SEI induced electrode offset. Rumpf et al. [66] addressed higher variation between batches than within. Differences in cell-to-cell variation could also be shown over a three-year production cycle in Schindler et al.'s [10] where three batches of cells were purchased 14-months apart. Results from most studies [61,65,66,68] showed that discharge capacities tend to follow and keep a normal distribution whereas the ones for polarization are skewed with a larger tail towards higher resistances. Schuster et al.'s study [68] found that, during aging, the distributions switch from normal to Weibull and assumed it was induced by interrelationship between the cell variations during the production process and the different aging mechanisms. Higher ctcV are expected for prototype cells and commercial cells with low volume production.

2.2.2. Cycling

Mechanically induced stress from the cycling can also cause inhomogeneities to arise. Through the charging and discharging regimes, Li^+ ions intercalation and deintercalation is often associated with volume changes which might lead to mechanical stresses. An advantage of cylindrical cells is high mechanical stability as their shape allows the even distribution of internal pressure. However, when the pressure build up is too high, the uniformity of the jelly roll can be compromised. Carter et al. [72] investigated mechanical failure in cylindrical cells by comparing cells with and without mandrels. At the pristine state, mandrel-less cells show less deformation than mandrel cells. However, the jelly roll in mandrel-less cells is shown to be more prone to mechanical collapse after cycling. Pfrang et al. [73] and Willenberg et al. [74] studied the morphology of the jelly roll of cylindrical cells. Pfrang et al. [73] noticed that the deformation almost always occurred between the PE tab and the inner pin. It was concluded that inhomogeneous architecture of the cells is caused mainly by the PE tab deformation which is the result of thickness variations of the NE and PE during charge/discharge cycles. Postmortem analysis showed delamination of the active material in the high stress area and the creation of gaps between the aluminum current collector and PE coating which contributed to the loss of active material. Willenberg et al. [74] correlates jelly roll deformations to cyclic aging, stating that, at the time of delivery, there were no signs of deformation. However, Bach et al. [12] noticed that even pristine cells exhibit signs of jelly roll deformation and linked the cause to the positioning of the tabs. The slight bulkiness of the tabs deforms the jelly roll and creates low and high-pressure areas also leading to separator inhomogeneities [75,76]. Lithium plating was mostly observed in high pressure areas. Mühlbauer et al. [77] focused on electrolyte distribution in cylindrical cells. Systematic results reveal lower lithium concentrations at the top and bottom of the aged cells possibly caused by mechanical deformities or inhomogeneous pressure or temperature gradients. Lower lithium concentrations were also observed in the outer region of cylindrical cells due to the inhomogeneous distribution of the liquid electrolyte [78,79].

The rigid case of prismatic cells helps them withstand high external mechanical stress situations; however, the folded sheets in the case experience high levels of internal stress especially at the edges. Coupled with manufacturing inhomogeneities, such as welding burrs, high internal stress can damage electrodes or cause uneven electrolyte distribution that can trigger unwanted lithium plating leading to internal short-circuits and thermal runaway. This happened to be the root cause of the well-known fire incident with the Samsung Galaxy Note 7 batteries [80,81] that is shown in Figure 4.

Figure 4. Observations of tab deformation and assembling and welding inconsistencies in the Samsung Galaxy Note 7 batteries: (**a**) X-ray CT scan of electrode deformation in the prismatic cell; (**b**) missing insulating tape on the cathode tabs; (**c**) SEM cross-section of an anode tab weld (CC BY Loveridge et al. [81]).

Several authors investigated temperature gradients across cells. Werner et al. [82] compared cell degradation under spatially homogeneous and inhomogeneous temperature distributions and observed different aging mechanisms between the two conditions. Uncontrolled inhomogeneous elevated temperatures can cause undesired side reactions that can accelerate degradation or result in thermal runaway [14]. Osswald et al. [83] used modified commercial cylindrical cells to study the influence of temperature on current distribution, leading to SOC inhomogeneities at different locations on the electrodes. The group recorded larger inhomogeneities for increasing temperatures and C-rates. Grandjean et al. [84] supports Osswald's findings in that thermal gradients increase with increasing C-rate and decreasing temperature. He also noted that the top of the pouch cell, where the tabs are located, is not the hottest area. A recent study by Carter et al. [85] on interelectrode thermal gradients demonstrated how they can induce certain battery degradation mechanisms. The electrochemical reactions within a cell are known to be highly temperature dependent; therefore, thermal gradients can create a capacity mismatch between the PE and NE and accelerate electrode degradation. Paarmann et al. [86] adds to this claim by stating that at lower temperatures, the same temperature difference has a higher impact on the current.

During their lifetime cells can be subject to various cycling—normal or abusive—conditions triggering certain degradation mechanisms that reveal themselves as inhomogeneities. This repeated process can initiate spatial inhomogeneities [87,88]. Gas formation is known to be a byproduct of electrolyte reduction [89]. Michalowski et al. [90] observed lower chemical activity in the center of a pouch cell and attributed it to a gas bubble creating a low pressure zone, reducing Li ion transport by poor contact. Similarly, in a pouch cell study performed by Devie et al. [91,92] where gas evolution was observed, they attributed the simultaneous loss of active material (LAM) on both electrodes to the interruption of the ionic conduction pathways between the PE and NE. Displacement of the gas bubble to the top of the stack allowed the inactive areas to become active again, regaining previously lost capacity.

The results from all of the above affect the cells and the impact of these variations is significant. In cells from the same production batch with little initial cell-to-cell variability, tested under the same testing conditions [61,93,94], inhomogeneities will arise and lead to large deviations from one another. Baumhöfer et al. [61] showed that aging 48 cells issued from the same production lot using an identical protocol resulted in large inhomogeneities with the worst cell having a cycle life 25% shorter than the best cell. In addition, little to no correlation was found between initial cell-to-cell variation and later degradation of the cells

during cycling [93,95]. For this reason, special attention must be exerted when dealing with battery pack assembly and highlights the need for accurate material-based state-of-health (SOH) estimation techniques [96].

2.3. Pack Level

Battery packs are often divided into multiple modules in series and/or in parallel and have a battery management system (BMS) to monitor performance. It is the final shape of the battery system that will be deployed for the chosen application. Such assemblies are necessary to meet rigorous power and energy requirements, and proper cell balancing as well as their appropriate connection are critical factors to monitor to prevent the rise of inhomogeneities. Cylindrical cells are usually welded to one another in large quantities allowing for simple construction. While space management remains somewhat suboptimal, the thermal management in a pack is easier due to the spaces between cells. It is one of the cheapest methods for producing large lithium-ion battery packs. Prismatic cell battery packs can store more energy within their volumes; thus they offer a higher energy density, and can be more powerful without using more space. The box-like shaped cases are ideal candidates for spatial optimization making the best use for available space but leaving limited room for proper thermal management. Pouch cells make the most efficient use of space because they do not have any metallic enclosure, but they are usually sensitive to external stress factors and therefore require alternative support during assembly.

Inhomogeneities in modules and packs can arise from several factors. Depending on the material properties and contact geometry of the battery casing and tabs, different welding techniques could be used to ensure proper connection between cells as well as proper assembly of battery packs. Brand et al. [97] presented an overview of three main welding techniques: resistance spot welding, ultrasonic welding and laser beam welding, with details on their influence on contact resistances in various types of batteries and battery casings. In all cases, heat was very localized which did not affect the health of the cells. Taylor et al. [98] discussed the effects of connectors and connections on the resistance of the circuit and, although the study was done for characterization experiments, their results are applicable and need to be taken into account. If done incorrectly, the integration of unmatched cells, poor cell connections or an asymmetric module design can lead to inhomogeneous currents flowing through the module [99] inducing temperature gradients leading to inhomogeneous degradation. Rumpf et al. [1] studied the influence of ctcV on the inhomogeneity of battery modules. The importance of a symmetric module design was highlighted in order to obtain symmetric current distribution. They also observed that an asymmetric design of cell connectors can have a larger impact on inhomogeneous current distribution than ctcV. Inhomogeneous current flow due to uneven contacts was also studied by Wang et al. [100]. They stated that inhomogeneous current flow through parallel cells is induced by the resistance of the intercell connecting plates. This caused cells to be discharged unevenly, therefore, lowering the terminal voltage of the module, affecting its usability. Offer et al. [101] backs the results of the previous studies by showing that uneven current flow in a pack is more likely to come from a defective intercell connection plate resistance rather than a cell with an abnormally high impedance. A pack containing 504 cells in a highly paralleled configuration was tested and it was shown that a single high intercell connection resistance was setting off large SOC variations between the cells in the same parallel strip, leading to the premature aging of the pack. A recent review on SOC estimation methods in lithium ion battery packs summarized the impact of cell inconsistencies due to manufacturing and welding processes on pack performance and SOC estimation [102].

The implementation of CtcV in battery pack models [103–105] helped show their impact on a multiscale level and they were found to have a much higher impact on cells connected in series rather than in parallel. Experimentally validated simulations by Liu et al. [106] placing a cell with a high internal impedance closest to the load where the currents are higher provide better cell-to-cell current distribution because higher internal

resistances lead to less current through the cell [107]. On other hand, placing a high internal impedance cell furthest from the load would be detrimental to the performance of the pack, reducing its capacity as the other lower impedance cells would get reach terminal voltage first. Neupert et al. [107] studied the current distribution depending on the position of cells with different impedances in a parallel configuration. Surprisingly, cell position in the parallel strip has a higher influence than the internal resistance of the cell at a specific position. Gogoana [63] linked resistance mismatch in parallel connected cells to capacity fade while Grün et al. [13] researched on the importance of the ratio of the cell's internal and contact resistances.

Liu et al. [106] and Wu et al. [108] observed that inhomogeneous current flow drives localized heat generation especially in cells closer to the load points of the pack. Dubarry et al. [109] used data from a deployed grid scale battery energy storage system containing more than 2500 batteries to examine temperature gradients between modules and found a maximum temperature variation of 16.5 °C between modules. Other studies have attempted to correlate capacity loss with temperature variations [110,111]. These thermal gradients could aggravate cell degradation and further accelerate the aging of the concerned cells, jeopardizing the performance and safety of the pack. Several other cell sorting studies were made in order to achieve better cell-to-cell consistency and push for longer cycle life [112,113]. Careful arrangement of cells in modules and modules in pack is primordial in assuring equal current flow throughout the module while minimizing thermal gradients, especially when high currents are in play. Cooling strategies are often thought off to help mitigate the effect of unwanted thermal gradients. Wang et al. [114] discussed multiple heat dissipation module configurations for cylindrical cells with and without forced air cooling and came to the conclusion that cubic structures are the best choice in terms of cooling capability as well as cost. The temperature distribution in the module also depends on the position and airflow of the cooling source. Cells nearer to the cooling source will inherently be cooler than those farther away. Effective heat dissipation and insulation technology are vital to adjust the temperature of the battery pack and help them reach their optimal operating temperature, reducing inhomogeneities while improving electrode kinetics.

All these variations will present the cells within a pack with different aging conditions which might exacerbate or inhibit certain degradation mechanisms. Although path dependence is not considered an inhomogeneity in itself, cells/modules following different degradation paths when they are supposed to be working homogeneously, can be considered inhomogeneous at the pack level. Path dependence poses an issue to predict aging of cells in a battery pack. These issues arise because cells are not subject to similar conditions all the time: variations in cell assembly, calendar aging between cells from different batches, thermal gradients, current distribution, etc. Several studies about path dependence [115–118] have been conducted. Results show that different cycling conditions induce different mixes of degradation mechanisms such as loss of lithium inventory (LLI), loss of active material at the negative electrode (LAM_{NE}) and loss of active material at the positive electrode (LAM_{PE}). The complex interaction between the different degrees of these losses will all lead to significantly different aging timelines. It is therefore, challenging to associate cell constant-current laboratory tests to sporadic driving conditions [119,120]. Path dependence is particularly notable when dealing with second life batteries as they have been already degraded over time [121,122]. Remanufacturing or refurbishing processes must ensure pack stability, but it can be challenging when the first life is not recorded.

3. Methods to Track Inhomogeneities

Inhomogeneities are a major concern for the reliability and safety of modern batteries. While significant effort must be deployed to eliminate them, developing advanced tracking methods to anticipate and quantify their impact is also crucial. A multitude of ways to track inhomogeneities can be found in the literature with different measuring principles and varying complexity. They differ in length scale from sub-particle to pack-to-pack

variance tracking, in time scales from milliseconds to years and in the complexity of the measurement instruments from particle accelerators down to using the onboard battery management system (BMS). In this section, a comprehensive set of analytical methods for evaluation of inhomogeneities and ctcV is presented. These methods are grouped by measurement complexity from research facility scale to laboratory scale and field scale methods, as depicted in Figure 5.
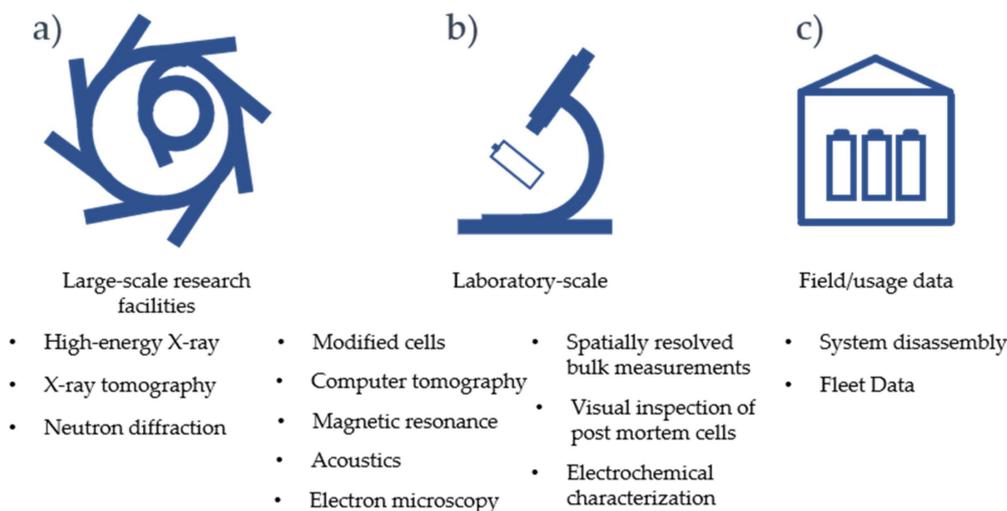

Figure 5. Different scales and complexity for ctcV and inhomogeneities measurements: (**a**) Large scale research facilities; (**b**) Laboratory-scale; (**c**) Field usage data.

3.1. Large-Scale Research Facilities

Large-scale research facilities generally allow for comprehensive investigations because they offer much higher brilliance for their spectroscopic measurements, a term that describes both the brightness and the angular spread of the beam. Synchrotron has brilliances more than a billion times larger than a standard laboratory X-ray source. Higher brilliances allow more resolution in measurements, to penetrate deeper into matter, to study much smaller features or to scan large area much faster.

3.1.1. High-Energy X-ray

High-energy X-ray (HEX) with energy levels over 80 keV can be used to nondestructively probe bulk processes on large format cells in situ and in operando [123]. To quantify inhomogeneities in situ Paxton et al. [59] used a polychromatic synchrotron X-ray source to perform energy-dispersive X-ray diffraction (EDXRD). Lithium cannot be tracked with this technique, but the lithiation dependent structure of the materials can be monitored. In [59], the distribution of the ratio of iron-phosphate $FePO_4$ to lithium-iron-phosphate $LiFePO_4$ at a particular region was used to track the local state of charge (SOC). It must be noted that with this technique, all sheets of the cell are measured at once and an average phase ratio is determined. An example of the determined phase ratios from [59] is presented in Figure 6a,b. The inhomogeneous discharge behavior is clearly visible as Locations C and F are not at the same SOC as the rest of the electrode.

3.1.2. X-ray Tomography

X-rays from synchrotrons can also be used for 3D-reconstruction of electrodes as performed by Müller et al. [24] with synchrotron radiation X-ray tomographic microscopy (SRXTM). Four commercial graphite anodes were measured on a μm-level and, amongst others, porosity, tortuosity, and particle size distributions were evaluated. In addition, this technique was used for determining the structure of silicon graphite negative electrodes

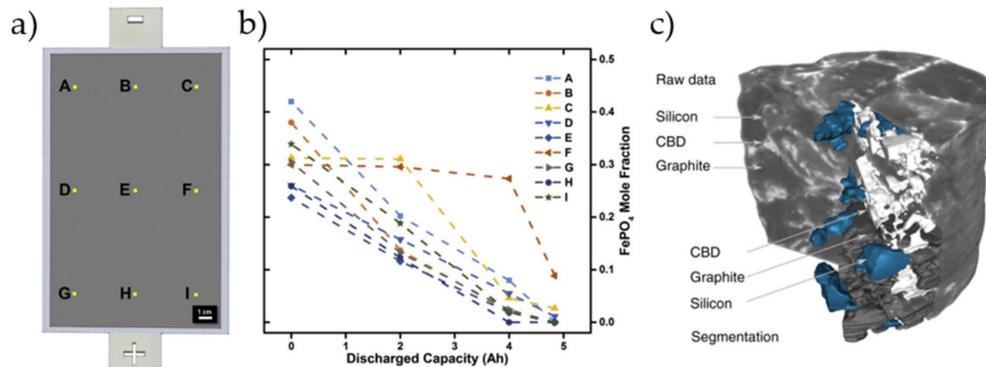and its 3D reconstructed in 3D [124]. An example of the obtainable reconstructions is presented in Figure 6c.

Figure 6. 3D reconstruction of electrodes: (**a**) Location of bulk measurement points, and (**b**) spatial inhomogeneity during discharge in LFP pouch cell. Reproduced with permission from [59] Copyright 2015, Elsevier. (**c**) The 3D-reconstruction of tomographic raw data and segmentation of silicon-graphite anode from a transmission X-ray tomographic microscope. Scale bar 15 μm. (CC BY 4.0 Müller et al. [124]).

3.1.3. Neutron Diffraction

Neutron diffraction offers advantages such as higher resolution for small atoms like lithium or the distinction between isotopes. Neutron reflections of the LiC_6 and LiC_{12} phases of graphite anodes also differ which can be used to approximate lithium concentration [79,125]. Since the measurement can be performed without destruction of the cell, the lithium distribution can be tracked during cell degradation [126–128]. With spatial resolution, this technique can be used in situ and 3D for example for determination of lithium distribution in cylindrical 18,650 full cells [129,130] as shown in Figure 7.
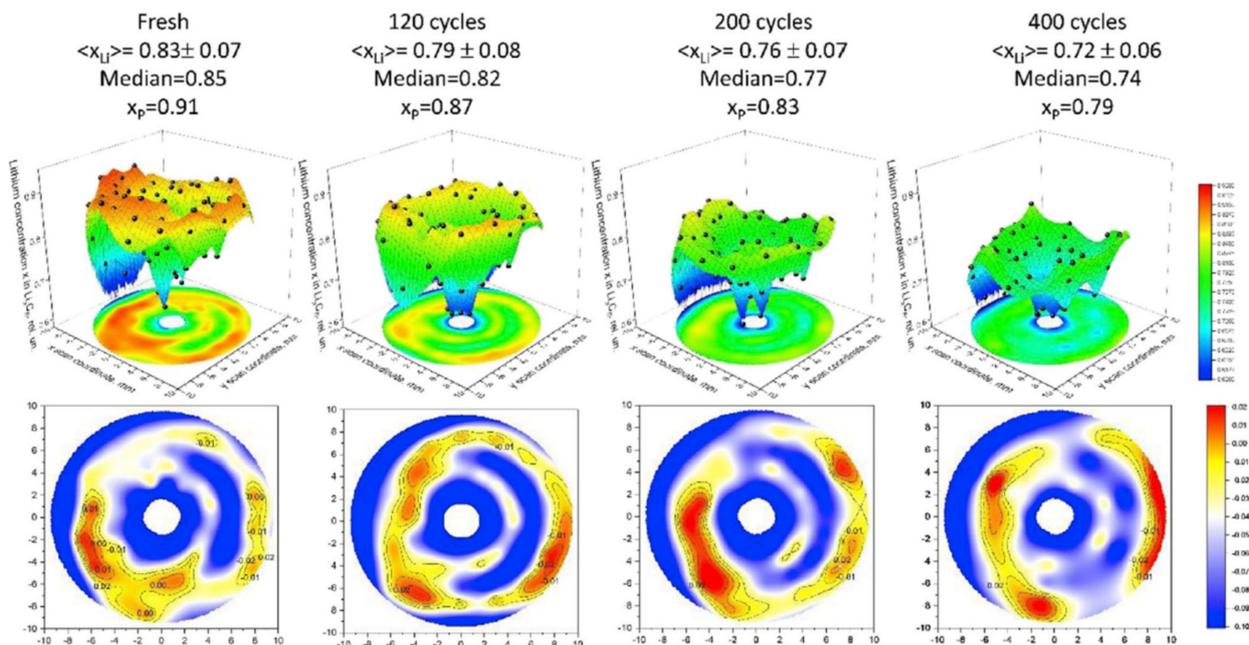

Figure 7. Lithium distribution as cross-section determined by differences of reflections of LiC6 and LiC12 phases in graphite with spatially resolved neutron diffraction. Over cycling inhomogeneities enhance. Reproduced with permission from [130] Copyright 2020, Elsevier.

3.2. Laboratory Scale Tracking

Compared to the very few research facilities with large instruments, laboratory scale devices and methods generally show much more widespread availability and can be performed in most battery research laboratories. In this subsection, laboratory scale approaches with specific focus on identification and characterization of inhomogeneities are presented. For a more general perspective on post-mortem techniques, the authors refer to Waldmann et al. [7], Lu et al. [8] and Harks et al. [9].

3.2.1. Cell Modifications

To investigate local variations in the internal state of a commercial cell, a widespread approach is modification and reconfiguration of the cell. Modification covers the introduction of sensors and reference electrodes into the cell. Fleming et al. placed temperature sensors inside a commercial cell to capture temperature gradients [131] while McTurk et al. [132] demonstrated the insertion of a wire reference electrode into a commercial pouch cell. Another approach was used by Osswald et al. [133] where the current tabs were separated and used to measure space-resolved electrochemical impedance spectroscopy (EIS) measurements as well as temperature changes during cycling [83]. Reconfiguration covers the extraction of single cell parts from a commercial cell, like one of the electrodes or the separator, and the reassembly of a new cell of new format (mostly coin cell format). This allows to evaluate the electrochemical behavior of aged samples whilst using reference compounds for all other parts. The new cell can then be evaluated as any other cell. Spatial resolution can be achieved by using samples from different regions of the commercial cell. In this context, Wang et al. [134] performed cycling tests and impedance measurements at coin cells obtained from different regions of a commercial 18,650 cell that aged inhomogeneous whereas Sieg et al. [20] created coin cells from a commercial pouch cell to evaluate local deviations in the differential voltage analysis caused by inhomogeneous lithium distribution and local cell aging. With the spatial resolution of the measurements aging maps of the electrode sheets were created, showing the location of aging gradients.

3.2.2. Spatially Resolved Bulk Measurements

Some of the measurement methods presented in this section are only capable of identifying bulk values for the whole sample introduced into the measurement, giving no opportunity to identify the spatial resolution of inhomogeneity within the sample. To apply these measurement methods for evaluation of inhomogeneity, units of interest for inhomogeneity (e.g., an electrode sheet) have to be subdivided into a set of samples that covers the area of the whole unit. These samples are then evaluated by bulk measurements independently. The spatial distribution of the samples hereby allows for the determination of the spatial resolution of the quantity measured by bulk measurements within the unit of interest. Sieg et al. [20] used this approach to determine the inhomogeneity of capacity distribution within a pouch cell by creating coin cells from an electrode pair and evaluating coin cell capacity. Figure 8 shows the spatial distribution of the samples (a), the optical changes on the anode (b) and the capacity distribution (c) for the electrode pair. Further spatially resolved bulk measurements were performed by Warnecke [135] by the use of inductively coupled plasma optical emission spectroscopy (IPC-OES) on different areas of the anodes to track inhomogeneous manganese distribution caused by manganese dissolution at the cathode.
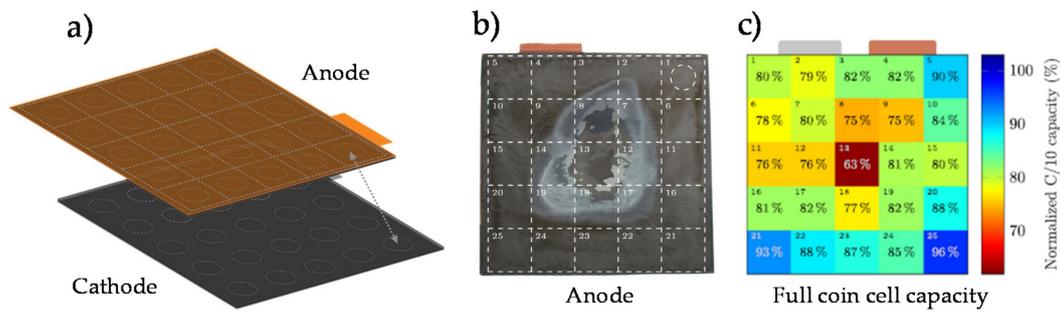
Figure 8. Spatially resolved capacity measurement with coin cells: (**a**) Shows schematic of the location of the samples; (**b**) Shows one anode sheet and sample locations; (**c**) Heat map with normalized C/10 capacity with location on the electrodes. Reproduced and modified with permission from [20] Copyright 2020, Elsevier.

3.2.3. Visual Inspection of Post-Mortem Cells

For qualitative evaluation of inhomogeneities within a cell, visual inspection of the electrodes and separator can be used to overview inhomogeneous cell behavior. Since graphite presents different colors depending on the lithiation stage, cells with graphite anodes can be inspected visually for inhomogeneous lithium distribution [136,137], an example from Spingler et al. [138] is presented in Figure 9a. In addition, lithium plating can be observed [28,139] as well as covering layers [140,141] and delamination [74]. Visual inspection of cell inhomogeneity can be further supported by means of light, as seen in Figure 9b where Käbitz [142] used laser microscopy in order to allow for higher degrees of magnification. Exemplarily, Ecker et al. [21] also applied laser microscopy for characterization of lithium plating in a commercial 40 Ah pouch cells.
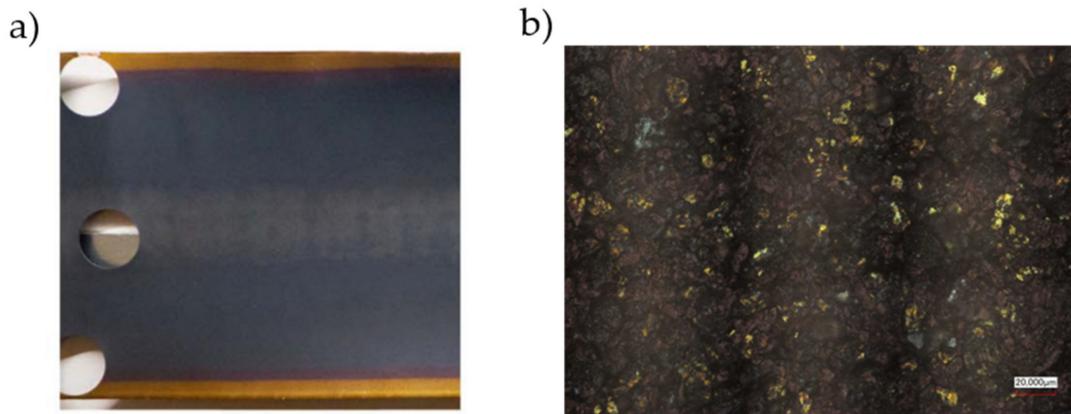

Figure 9. Visual inspection of electrodes: (**a**) Part of the anode of an 18,650 cell with coin cell probes taken in different locations of the cell. The outer part of the electrode shows a different lithiation than the middle part. (Modified from CC BY 4.0 by Spingler et al. [138]); (**b**) optical microscopy of the outer part of an anode showing individual particles with different lithiation (CC BY 4.0 by Käbitz [142]).

3.2.4. Electron Microscopy

Compared to light microscopy, scanning electron microscopy (SEM) allows for higher magnification and can track inhomogeneities on a material level. This includes uneven particle sizes, particle cracking, delamination [81] or deformation [143]. Whilst SEM is not capable to penetrate into active materials, focused ion beam milling (FIB) can be applied to erode the active material layer by layer and allow for 3D-imaging of electrode structures using FIB/SEM [124]. Furthermore, SEM can be coupled with an energy-dispersive X-ray spectroscopy detector (EDX) to allow for spatially resolved determination of elemental composition in the active material. Burow et al. [144] applied SEM/EDX to detect inhomogeneous lithium plating in automotive cells cycled at low temperatures.

3.2.5. Computer Tomography

Computer tomography (CT) uses X-rays and moving sample to reconstruct a 3D representation of the cell. On the laboratory scale it can be used with lower resolution (up to 100 µm resolution) for full cells, as well as for parts of a cell with higher resolution. The main field of application for CT is the non-destructive geometric depiction of the cell. This allows for the spatially resolved identification of deformations that can be caused by uneven stress within the battery or by delamination. Computer tomography has shown multiple times the deformation of the jelly roll in cylindrical cells [72–74,142,144]. On a nanoscale, CT can also be used to see heterogenous particle cracking and covering layer formation [145,146]. Li and Hou also reported correlation between their capacity measurements and CT image data [147].

3.2.6. Magnetic Resonance

Magnetic resonance spectroscopy techniques enable the identification of material compositions inside of lithium-ion batteries. This allows for the identification of phase compositions and active and passive materials degradation due to cell aging. The magnetic susceptibilities of many cathode materials depend upon their lithiation state [148]. Ilott et al. used magnetic resonance imaging (MRI) on small 600 mAh pouch cells with an induced magnetic field being changed as a function of state of charge [148]. With various magnetic field maps taken at different charge levels, inhomogeneous lithium distribution within the cell could be found. In addition, defective cells could be identified. While MRI is using the intensity of radiation, nuclear magnetic resonance (NMR) does analyze the frequency of the response signal. Krachkovskiy signatures from stages of graphite lithiation can be seen in NMR spectra [149]. Furthermore, NMR can be applied for identification of electrolyte decomposition as shown by Wiemers-Meyer et al. [150]

3.2.7. Acoustics

Acoustic measurements can be used to gain information on the geometric structure inside a cell and on the composition and lithiation of the active materials. The acoustic properties of electrode materials correlate with state of charge due to changes in the density during lithiation. Using this property, differences in lithiation during usage were mapped by Robinson et al. in small pouch cells with spatially resolved ultrasound measurements coupled CT measurements [88]. Bauermann et al. showed scanning acoustic microscopy (SAM) can visualize defects inside battery cells non-destructively. With distinct acoustic impedances inhomogeneities are detected and localized. SAM is best used on flat and thin battery cells and on effects like gas formation with high sensibility of the acoustic patterns [151]. Acoustic attenuation spectroscopy (AAS) can be used to determine the particle size distribution post mortem by dissolving binders in electrode samples thus transforming the active material into a particle suspension [26].

3.2.8. Electrochemical Characterization

Unlike many of the aforementioned methods, electrochemical characterization can be performed directly on the commercial cells with no need for cell opening nor sample extraction to generate a bulk information about the full cell. Moreover, it can also be performed on electrode cutouts, as mentioned in the Section 3.2.1, to allow spatially resolved analysis of the electrochemical cell behavior. Electrochemical measurements allow to gather information on the thermodynamic state of the cell as well as its kinetics.

CtcV are usually characterized during a conditioning test at the beginning of testing [152]. In addition, those measurements are part of every aging study and can reveal cell-to-cell variation over the lifetime of a cell [93,94]. One such experiment is shown in Figure 10a from Baumhöfer et al. with 48 cells cycled under equal conditions. This test usually involves the assessment of the distribution of capacity, rate capability, and resistance [10,61–66] to assess thermodynamic and kinetic variations. For a capacity test, the cells are usually fully charged and then discharged to the end-of-discharge-voltage

by a defined current. The integral of the discharge current over the discharge time is the resulting cell capacity and depends on the applied C-rate but converges to the theoretical cell capacity for low C-rates. Rate capability can be characterized by the Peukert constant or a ratio of two different rates [152]. For the characterization of resistance, the voltage drop associated with the application of current could be used, or the cell can be excited by short high-current pulses with various defined frequencies (electrochemical impedance spectroscopy) but this requires specific equipment. Electrochemical impedance spectroscopy also allows for the distinction of electrochemical processes within the cell associated with different relaxation time constants. Thereby, variations in conductivities, charge transfer reactions, and diffusion behavior can be investigated independently. If no equivalent circuit model is available, an investigation of the distribution of relaxation times (DRT) also allows for the characterization of ctcV. An overview over electrochemical impedance spectroscopy for lithium ion batteries is presented by Meddings et al. [153].
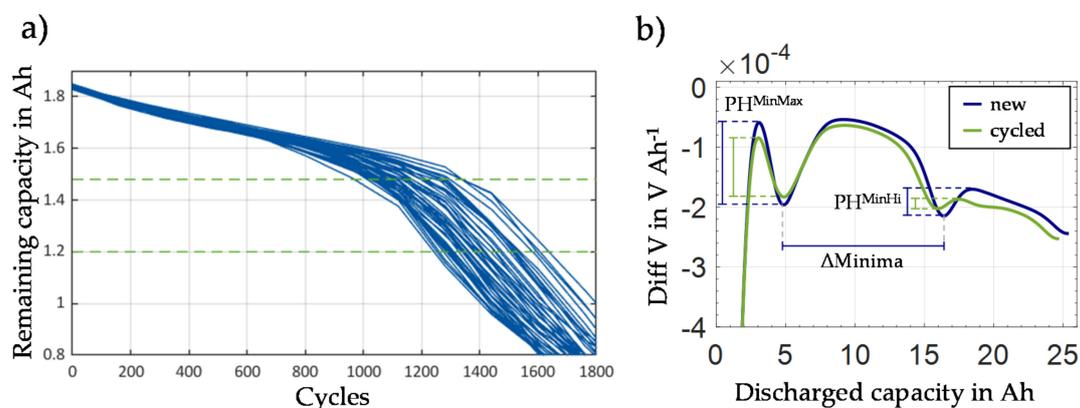

Figure 10. Different aging trends and differential voltage analysis: (**a**) The 48 cells under equal conditions with focus on inherent production caused cell-to-cell variance and capacity degradation over cycles, 80% and 60% of initial capacity are marked with green dashed line. Reproduced from Baumhöfer et al. [61]. (**b**) Differential voltage analysis on a 25 Ah cell to determine changes in the peak heights to quantify the homogeneity of lithium distribution [126].

Lastly, the use of electrochemical voltage spectroscopies, differential voltage analysis (DVA) [154], and incremental capacity analysis (ICA) [155] were also shown to allow the visualization of ctcV. Inhomogeneities are harder to assess at the full cell level because of the bulk nature of the measurements. However, DVA and ICA were shown to offer strong insight. Lewerenz et al. [156] observed some valley broadening using DVA, 10b, and associated them with growing inhomogeneities. If parts of the electrodes have a higher charge level due to an inhomogeneous lithium distribution, those areas will show the peaks in the DVA later during a constant discharge [156]. As the overall voltage corresponds to all individual voltages, the steps in the discharge curve and peaks in the DVA should be less prominent in inhomogeneous cells. ICA and DVA can also be used to visualize differences within cells in modules or packs [104,157–160].

Another indicator for homogeneity within a cell or packs can be evaluated by tracking differences in rate capability over time [155,161]. For this technique, the difference of rate capability, i.e., the extractable capacity at a certain current, could be monitored for at least two current rates. A substantial increase of the difference of both capacities infers that parts of the active material are less accessible with high currents [161]. When applying this approach, it is necessary to verify that the resulting differences in rate capability are not just linked to an increase in resistance and to the rising overvoltage of successive discharges in the check-ups of the aging test [152].

3.2.9. Characterization of Inhomogeneous Cell Degradation

As discussed in detail in Section 2.2.2, cell inhomogeneity can be strongly related to cell aging and degradation. Thus, inhomogeneities, as a result of typical cell degradation

processes, can be quantified by the application of localized post-mortem methods for inspection of cell aging phenomena that were presented in this section. Electrochemical characterization methods are best fitted for characterization of ctcV with further possibilities to also investigate internal inhomogeneities by cell modification, spatially resolved bulk measurements and DVA/ICA. In contrast, the presented methods for visual inspection, spectroscopy and tomography are mostly applied for the characterization of inhomogeneities within a cell such as lithium distribution and local degradation phenomena. Figure 11 illustrates the feasibility for detection of different degradation phenomena for the established post-mortem measurement procedures presented in this section. Furthermore, the spatial resolution of the measurement referred to as sensitivity is evaluated, indicating whether spatially resolved bulk measurements have to be performed in order to assess inhomogeneity.

Method	cell inhomogeneities	cell-to-cell variation	sensitivity	Cell level degradation			Electrode/separator degradation			Material degradation		
				loss of active material	loss of lithium inventory	rise of inner resistance	growth of films on electrodes	clogging of pores	delamination of electrode separator	changes/films on particle surfaces	particle cracks/exfoliation	dissolution/migration of transition metals
Optical microscopy	yes	limited	surface	no	no	limited	yes	limited	yes	no	no	no
SEM	yes	limited	surface	no	no	yes	yes	yes	yes	yes	yes	no
EDX	yes	limited	surface	no	no	yes	yes	yes	no	yes	no	yes
XPS	yes	limited	surface	no	no	yes	yes	no	no	yes	no	no
ICP-OES	yes	limited	bulk	no	yes	no	no	no	no	no	no	yes
NMR	yes	limited	bulk	no	limited	no	no	no	no	no	yes	yes
XRD	yes	limited	bulk	limited	no	no	no	no	no	limited	no	no
electrochemical	limited	yes	bulk	yes	yes	yes	yes	limited	yes	no	yes	yes

Legend: yes | limited | no

Figure 11. Post-mortem analysis methods (modified from Waldmann et al., 2016 CC BY 4.0 [7]).

3.3. Field/Usage Data

Whilst laboratory scale measurements rely on destructive, ex situ or in situ experiments with preselected cells detached from their commercial application, field and usage data can be directly utilized in operando with no need for further experimental efforts [162]. A metric for homogeneity commonly tracked from large sets of field data is the capacity variation in between batteries, either tracked within the application or afterwards. This data is highly interesting for assessing the real-world degradation behavior of batteries without accelerated aging and with more variance on the stress factors such as climate or usage profile. Many manufacturers log data from their battery systems, but this data is rarely presented [163] and not published to the best knowledge of the authors. The battery community would greatly benefit from the release of large datasets.

3.3.1. Usage Data

In Liaw et al. [120], trip data from 18 vehicles was recorded and analyzed for the specific use of each vehicle and differences in climate and other stress factors on the battery. For in-depth data on inhomogeneities within a battery pack, disassembly and measurement of each component are possible. Schuster et al. [68] dissembled two vehicle battery packs and tested the capacity of aged 954 cells and compared them to 484 new ones. On a smaller scale, 152 notebook batteries with a total of 1034 cells were dissembled by Salinas et al. [164] reading the capacity, manufacturing date and cycle count for each cell from the BMS chip. To the authors' knowledge, system disassembly has only been reported for at most a few

large-scale battery systems, giving a good inside of cell-to-cell variance within the specific pack but not for the variation in between multiple packs.

3.3.2. Consumer Reports

There are several consumer reports of the state of battery systems especially for electric vehicles [139–141]. In the maximal range survey performed by the Tesla Motors Club in the Netherlands, participants record several parameters about their private EV, including depicted range, mileage and vehicle age. In Figure 13, the capacity degradation is shown up to six years and 200,000 km with some individual vehicles included at multiple times. A general degradation trend and longevity of the battery packs can be seen but effects from stress as the temperature profile of an individual pack are not included.

Since consumer reports are voluntary, typically the participants are well informed and highly interested. This bias towards well caring consumers may only reflect a sub portion of users with less variability. Another major drawback of consumer reports is the type of data collected. Typically, either the state-of-health value estimated by the BMS depicted on the driver's screen or the range after a full charge is recorded manually along the mileage. The SOH algorithm's function is unknown to the public and can be changed in between measurements with an update, invalidating data collected previously since values are not comparable anymore [165]. In addition, as explained in Figure 12, the user typically can only see the net capacity and therefore will only see degradation in the driver's display when the reserve is already degraded.
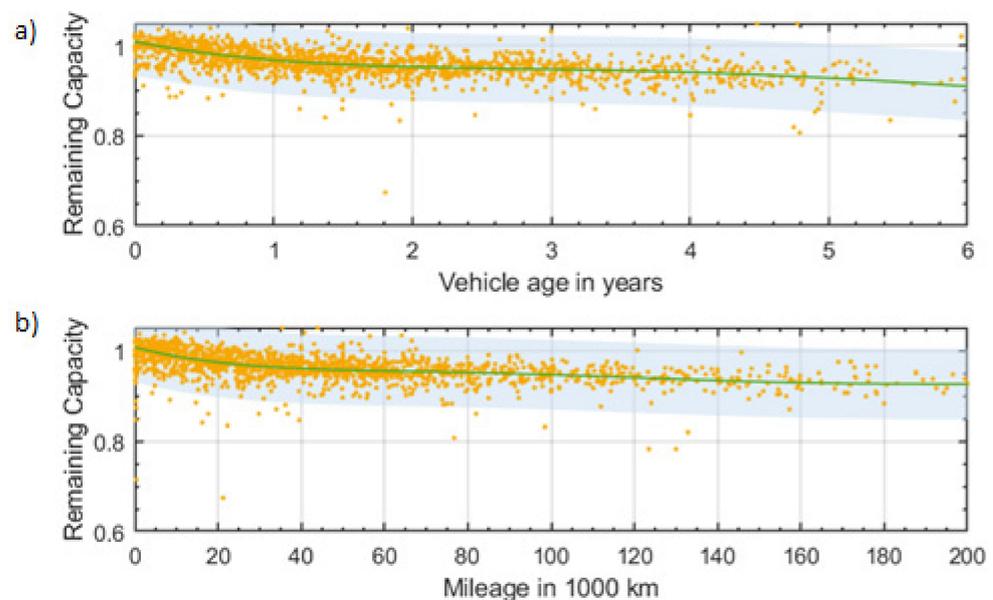

Figure 12. Maximal range survey from Tesla Motors, Netherlands forum with reported remaining capacity over: (**a**) years and (**b**) mileage from [166]. Each orange dot is one entrance and vehicles can have multiple entries within their life. The trendline is shown in green and 95% confidence interval in light blue.

Range estimators as a measurement for capacity also include the driver's energy efficiency level. Comparing multiple cars will not only reflect the different degradation levels, but also driver-to-driver variability. The depicted range for an energy intensive driver at the fully charged state at the same degradation level will be lower compared to an energy efficient driver. Another variability unconnected to the battery itself is the energy needed for cooling in hot climate included in the energy consumption. This granular data, if collected, is not available through consumer reports.
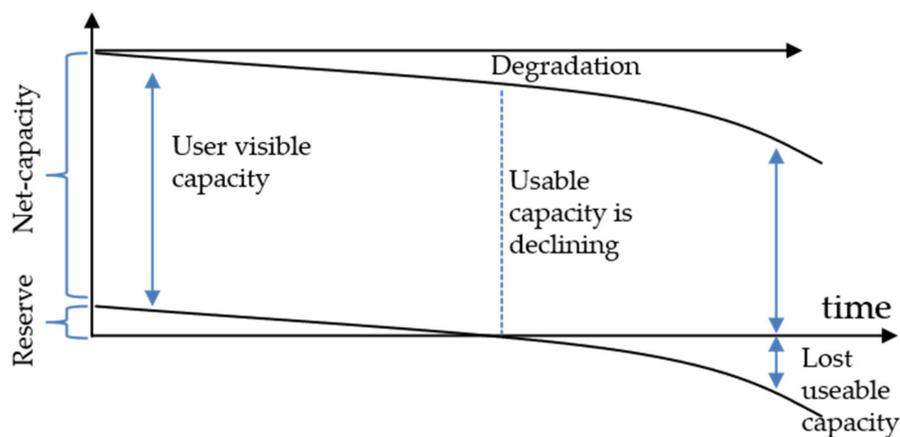
Figure 13. User visible capacity from battery management system, reserve is not shown to the user but the state-of-health remains 100% even though degradation already happened.

4. Conclusions and Outlook

This review summarized the origins of the inhomogeneities as well as the various methods used to track variations and inhomogeneities with their value and effectiveness at their respective scale.

Inhomogeneities in lithium-ion batteries are a well-known performance and safety altering issue. Cell-to-cell variations and inhomogeneities arise not only from different aging conditions but also from disparities in chemistry, materials, processing, cell format, and connectors. Multiple studies have been conducted on a multiscale level and evidence of inhomogeneous degradation was obtained using complex mapping techniques (Raman spectroscopy, X-ray and neutron diffraction, tomography, laser scanning), post-mortem studies using electrochemical tests, scanning electron microscopy (SEM), and X-ray diffraction (XRD), or from the sensors available in the field. However, this tracking is resource intensive and ctcV and reproducibility are unfortunately not addressed in all studies. We believe every study testing multiple samples or cells should report on ctcV. Taking the example of electrochemical testing, this could be easily done with a standardized quick check test included in the conditioning step. In addition, all experiments should be systematically replicated so that variations upon aging could be quantified. This information is drastically needed to be able to correctly model cell performance in assemblies.

Looking at the final application, and the deployment of more and more large batteries in the field, we believe that taking ctcV and inhomogeneities into consideration is what is currently lacking in BMS because of the lack of in operando methods. Even if progress in manufacturing will keep lowering the standard deviations between cells, tracking inhomogeneities will undoubtedly play an essential role in future BMS to be able to forecast performance and durability. This implies that new methods are needed to be able to quantify them nondestructively, which eliminates most of the methods mentioned above. Electrochemical voltage spectroscopies appear, so far, to be the best candidates for the task, however, more studies and a fundamental understanding are needed to reach quantitative rather than qualitative deductions.

Author Contributions: Conceptualization, M.D., D.U.S. and P.D.; methodology, D.B., P.D. and M.D.; software, D.B., P.D. and M.D.; validation, D.B., P.D., M.J. and M.D.; formal analysis, D.B., P.D. and M.D.; investigation, D.B., P.D. and M.D.; resources, P.D. and M.D.; data curation, D.B., P.D., M.J. and M.D.; writing—original draft preparation, D.B., P.D. and M.D.; writing—review and editing, all authors; visualization, D.B. and P.D.; supervision, M.D. and D.U.S.; funding acquisition, M.D., P.D. and D.U.S. All authors have read and agreed to the published version of the manuscript.

References

1. Rumpf, K.; Rheinfeld, A.; Schindler, M.; Keil, J.; Schua, T.; Jossen, A. Influence of Cell-to-Cell Variations on the Inhomogeneity of Lithium-Ion Battery Modules. *J. Electrochem. Soc.* **2018**, *165*, A2587–A2607. [CrossRef]
2. Palacin, M.R. Battery Materials Design Essentials. *Acc. Mater. Res.* **2021**. [CrossRef]
3. Liu, H.; Cheng, X.; Chong, Y.; Yuan, H.; Huang, J.-Q.; Zhang, Q. Advanced Electrode Processing of Lithium Ion Batteries: A Review of Powder Technology in Battery Fabrication. *Particuology* **2021**, *57*, 56–71. [CrossRef]
4. Xiong, R.; Pan, Y.; Shen, W.; Li, H.; Sun, F. Lithium-Ion Battery Aging Mechanisms and Diagnosis Method for Automotive Applications: Recent Advances and Perspectives. *Renew. Sustain. Energy Rev.* **2020**, *131*, 110048. [CrossRef]
5. Pastor-Fernández, C.; Yu, T.F.; Widanage, W.D.; Marco, J. Critical Review of Non-Invasive Diagnosis Techniques for Quantification of Degradation Modes in Lithium-Ion Batteries. *Renew. Sustain. Energy Rev.* **2019**, *109*, 138–159. [CrossRef]
6. Boebinger, M.G.; Lewis, J.A.; Sandoval, S.E.; McDowell, M.T. Understanding Transformations in Battery Materials Using in Situ and Operando Experiments: Progress and Outlook. *ACS Energy Lett.* **2020**, *5*, 335–345. [CrossRef]
7. Waldmann, T.; Iturrondobeitia, A.; Kasper, M.; Ghanbari, N.; Aguesse, F.; Bekaert, E.; Daniel, L.; Genies, S.; Gordon, I.J.; Löble, M.W.; et al. Review—Post-Mortem Analysis of Aged Lithium-Ion Batteries: Disassembly Methodology and Physico-Chemical Analysis Techniques. *J. Electrochem. Soc.* **2016**, *163*, A2149–A2164. [CrossRef]
8. Lu, J.; Wu, T.; Amine, K. State-of-the-Art Characterization Techniques for Advanced Lithium-Ion Batteries. *Nat. Energy* **2017**, *2*, 17011. [CrossRef]
9. Harks, P.P.R.M.L.; Mulder, F.M.; Notten, P.H.L. In Situ Methods for Li-Ion Battery Research: A Review of Recent Developments. *J. Power Sources* **2015**, *288*, 92–105. [CrossRef]
10. Schindler, M.; Sturm, J.; Ludwig, S.; Schmitt, J.; Jossen, A. Evolution of Initial Cell-to-Cell Variations During a Three-Year Production Cycle. *eTransportation* **2021**, 100102. [CrossRef]
11. Harris, S.J.; Lu, P. Effects of Inhomogeneities—Nanoscale to Mesoscale—On the Durability of Li-Ion Batteries. *J. Phys. Chem. C* **2013**, *117*, 6481–6492. [CrossRef]
12. Bach, T.C.; Schuster, S.F.; Fleder, E.; Müller, J.; Brand, M.J.; Lorrmann, H.; Jossen, A.; Sextl, G. Nonlinear Aging of Cylindrical Lithium-Ion Cells Linked to Heterogeneous Compression. *J. Energy Storage* **2016**, *5*, 212–223. [CrossRef]
13. Grün, T.; Stella, K.; Wollersheim, O. Influence of Circuit Design on Load Distribution and Performance of Parallel-Connected Lithium Ion Cells for Photovoltaic Home Storage Systems. *J. Energy Storage* **2018**, *17*, 367–382. [CrossRef]
14. Ma, S.; Jiang, M.; Tao, P.; Song, C.; Wu, J.; Wang, J.; Deng, T.; Shang, W. Temperature Effect and Thermal Impact in Lithium-Ion Batteries: A Review. *Prog. Nat. Sci. Mater. Int.* **2018**, *28*, 653–666. [CrossRef]
15. Nguyen, T.-T.; Demortière, A.; Fleutot, B.; Delobel, B.; Delacourt, C.; Cooper, S.J. The Electrode Tortuosity Factor: Why the Conventional Tortuosity Factor Is Not Well Suited for Quantifying Transport in Porous Li-Ion Battery Electrodes and What to Use Instead. *NPJ Comput. Mater.* **2020**, *6*, 123. [CrossRef]
16. Forouzan, M.M.; Chao, C.-W.; Bustamante, D.; Mazzeo, B.A.; Wheeler, D.R. Experiment and Simulation of the Fabrication Process of Lithium-Ion Battery Cathodes for Determining Microstructure and Mechanical Properties. *J. Power Sources* **2016**, *312*, 172–183. [CrossRef]
17. Thorat, I.V.; Stephenson, D.E.; Zacharias, N.A.; Zaghib, K.; Harb, J.N.; Wheeler, D.R. Quantifying Tortuosity in Porous Li-Ion Battery Materials. *J. Power Sources* **2009**, *188*, 592–600. [CrossRef]
18. Antartis, D.; Dillon, S.; Chasiotis, I. Effect of Porosity on Electrochemical and Mechanical Properties of Composite Li-Ion Anodes. *J. Compos. Mater.* **2015**, *49*, 1849–1862. [CrossRef]
19. Elango, R.; Nadeina, A.; Cadiou, F.; De Andrade, V.; Demortière, A.; Morcrette, M.; Seznec, V. Impact of Electrode Porosity Architecture on Electrochemical Performances of 1 Mm-Thick LiFePO4 Binder-Free Li-Ion Electrodes Fabricated by Spark Plasma Sintering. *J. Power Sources* **2021**, *488*, 229402. [CrossRef]
20. Sieg, J.; Storch, M.; Fath, J.; Nuhic, A.; Bandlow, J.; Spier, B.; Sauer, D.U. Local Degradation and Differential Voltage Analysis of Aged Lithium-Ion Pouch Cells. *J. Energy Storage* **2020**, *30*, 101582. [CrossRef]
21. Ecker, M.; Shafiei Sabet, P.; Sauer, D.U. Influence of Operational Condition on Lithium Plating for Commercial Lithium-Ion Batteries—Electrochemical Experiments and Post-Mortem-Analysis. *Appl. Energy* **2017**, *206*, 934–946. [CrossRef]

22. Suthar, B.; Northrop, P.W.C.; Rife, D.; Subramanian, V.R. Effect of Porosity, Thickness and Tortuosity on Capacity Fade of Anode. *J. Electrochem. Soc.* **2015**, *162*, A1708. [CrossRef]
23. Singh, M.; Kaiser, J.; Hahn, H. Effect of Porosity on the Thick Electrodes for High Energy Density Lithium Ion Batteries for Stationary Applications. *Batteries* **2016**, *2*, 35. [CrossRef]
24. Müller, S.; Eller, J.; Ebner, M.; Burns, C.; Dahn, J.; Wood, V. Quantifying Inhomogeneity of Lithium Ion Battery Electrodes and Its Influence on Electrochemical Performance. *J. Electrochem. Soc.* **2018**, *165*, A339–A344. [CrossRef]
25. Dubarry, M.; Gaubicher, J.; Guyomard, D.; Steunou, N.; Livage, J.; Dupré, N.; Grey, C.P. Synthesis of Li1+αV3O8 via a Gel Precursor: Part II, from Xerogel to the Anhydrous Material. *Chem. Mater.* **2006**, *18*, 629–636. [CrossRef]
26. Pavoni, F.H.; Sita, L.E.; dos Santos, C.S.; da Silva, S.P.; da Silva, P.R.C.; Scarminio, J. $LiCoO_2$ Particle Size Distribution as a Function of the State of Health of Discarded Cell Phone Batteries. *Powder Technol.* **2018**, *326*, 78–83. [CrossRef]
27. Yang, L.; Chen, H.-S.; Song, W.-L.; Fang, D. Effect of Defects on Diffusion Behaviors of Lithium-Ion Battery Electrodes: In Situ Optical Observation and Simulation. *ACS Appl. Mater. Interfaces* **2018**, *10*, 43623–43630. [CrossRef] [PubMed]
28. Liu, X.M.; Fang, A.; Haataja, M.P.; Arnold, C.B. Size Dependence of Transport Non-Uniformities on Localized Plating in Lithium-Ion Batteries. *J. Electrochem. Soc.* **2018**, *165*, A1147–A1155. [CrossRef]
29. Pouraghajan, F.; Thompson, A.I.; Hunter, E.E.; Mazzeo, B.; Christensen, J.; Subbaraman, R.; Wray, M.; Wheeler, D. The Effects of Cycling on Ionic and Electronic Conductivities of Li–Ion Battery Electrodes. *J. Power Sources* **2021**, *492*, 229636. [CrossRef]
30. Forouzan, M.M.; Mazzeo, B.A.; Wheeler, D.R. Modeling the Effects of Electrode Microstructural Heterogeneities on Li-Ion Battery Performance and Lifetime. *J. Electrochem. Soc.* **2018**, *165*, A2127–A2144. [CrossRef]
31. Vogel, J.E.; Forouzan, M.M.; Hardy, E.E.; Crawford, S.T.; Wheeler, D.R.; Mazzeo, B.A. Electrode Microstructure Controls Localized Electronic Impedance in Li-Ion Batteries. *Electrochim. Acta* **2019**, *297*, 820–825. [CrossRef]
32. Zhou, W. Effects of External Mechanical Loading on Stress Generation during Lithiation in Li-Ion Battery Electrodes. *Electrochim. Acta* **2015**, *185*, 28–33. [CrossRef]
33. Christensen, J. Modeling Diffusion-Induced Stress in Li-Ion Cells with Porous Electrodes. *J. Electrochem. Soc.* **2010**, *157*, A366. [CrossRef]
34. Lin, N.; Jia, Z.; Wang, Z.; Zhao, H.; Ai, G.; Song, X.; Bai, Y.; Battaglia, V.; Sun, C.; Qiao, J.; et al. Understanding the Crack Formation of Graphite Particles in Cycled Commercial Lithium-Ion Batteries by Focused Ion Beam—Scanning Electron Microscopy. *J. Power Sources* **2017**, *365*, 235–239. [CrossRef]
35. Dai, K.; Wang, Z.; Ai, G.; Zhao, H.; Yuan, W.; Song, X.; Battaglia, V.; Sun, C.; Wu, K.; Liu, G. The Transformation of Graphite Electrode Materials in Lithium-Ion Batteries after Cycling. *J. Power Sources* **2015**, *298*, 349–354. [CrossRef]
36. Sun, F.; Markötter, H.; Dong, K.; Manke, I.; Hilger, A.; Kardjilov, N.; Banhart, J. Investigation of Failure Mechanisms in Silicon Based Half Cells during the First Cycle by Micro X-Ray Tomography and Radiography. *J. Power Sources* **2016**, *321*, 174–184. [CrossRef]
37. Wu, H.; Cui, Y. Designing Nanostructured Si Anodes for High Energy Lithium Ion Batteries. *Nano Today* **2012**, *7*, 414–429. [CrossRef]
38. Wu, H.; Zheng, G.; Liu, N.; Carney, T.J.; Yang, Y.; Cui, Y. Engineering Empty Space between Si Nanoparticles for Lithium-Ion Battery Anodes. *Nano Lett.* **2012**, *12*, 904–909. [CrossRef] [PubMed]
39. Wang, D.; Wu, X.; Wang, Z.; Chen, L. Cracking Causing Cyclic Instability of LiFePO4 Cathode Material. *J. Power Sources* **2005**, *140*, 125–128. [CrossRef]
40. Gabrisch, H.; Wilcox, J.; Doeff, M.M. TEM Study of Fracturing in Spherical and Plate-like LiFePO4 Particles. *Electrochem. Solid State Lett.* **2008**, *11*, A25. [CrossRef]
41. Birkl, C.R.; Roberts, M.R.; McTurk, E.; Bruce, P.G.; Howey, D.A. Degradation Diagnostics for Lithium Ion Cells. *J. Power Sources* **2017**, *341*, 373–386. [CrossRef]
42. Dubarry, M.; Truchot, C.; Liaw, B.Y. Cell Degradation in Commercial LiFePO4 Cells with High-Power and High-Energy Designs. *J. Power Sources* **2014**, *258*, 408–419. [CrossRef]
43. Schmidt, O.; Thomitzek, M.; Röder, F.; Thiede, S.; Herrmann, C.; Krewer, U. Modeling the Impact of Manufacturing Uncertainties on Lithium-Ion Batteries. *J. Electrochem. Soc.* **2020**, *167*, 060501. [CrossRef]
44. Higa, K.; Zhao, H.; Parkinson, D.Y.; Barnard, H.; Ling, M.; Liu, G.; Srinivasan, V. Electrode Slurry Particle Density Mapping Using X-ray Radiography. *J. Electrochem. Soc.* **2017**, *164*, A380. [CrossRef]
45. Lenze, G.; Bockholt, H.; Schilcher, C.; Froböse, L.; Jansen, D.; Krewer, U.; Kwade, A. Impacts of Variations in Manufacturing Parameters on Performance of Lithium-Ion-Batteries. *J. Electrochem. Soc.* **2018**, *165*, A314–A322. [CrossRef]
46. Dreger, H.; Haselrieder, W.; Kwade, A. Influence of Dispersing by Extrusion and Calendering on the Performance of Lithium-Ion Battery Electrodes. *J. Energy Storage* **2019**, *21*, 231–240. [CrossRef]
47. Kenney, B.; Darcovich, K.; MacNeil, D.D.; Davidson, I.J. Modelling the Impact of Variations in Electrode Manufacturing on Lithium-Ion Battery Modules. *J. Power Sources* **2012**, *213*, 391–401. [CrossRef]
48. Rynne, O.; Dubarry, M.; Molson, C.; Nicolas, E.; Lepage, D.; Prébé, A.; Aymé-Perrot, D.; Rochefort, D.; Dollé, M. Exploiting Materials to Their Full Potential, a Li-Ion Battery Electrode Formulation Optimization Study. *ACS Appl. Energy Mater.* **2020**, *3*, 2935–2948. [CrossRef]
49. Mauler, L.; Duffner, F.; Leker, J. Economies of Scale in Battery Cell Manufacturing: The Impact of Material and Process Innovations. *Appl. Energy* **2021**, *286*, 116499. [CrossRef]

50. Haselrieder, W.; Ivanov, S.; Christen, D.K.; Bockholt, H.; Kwade, A. Impact of the Calendering Process on the Interfacial Structure and the Related Electrochemical Performance of Secondary Lithium-Ion Batteries. *ECS Trans.* **2013**, *50*, 59–70. [CrossRef]
51. Ngandjong, A.C.; Lombardo, T.; Primo, E.N.; Chouchane, M.; Shodiev, A.; Arcelus, O.; Franco, A.A. Investigating Electrode Calendering and Its Impact on Electrochemical Performance by Means of a New Discrete Element Method Model: Towards a Digital Twin of Li-Ion Battery Manufacturing. *J. Power Sources* **2021**, *485*, 229320. [CrossRef]
52. Kang, H.; Lim, C.; Li, T.; Fu, Y.; Yan, B.; Houston, N.; De Andrade, V.; De Carlo, F.; Zhu, L. Geometric and Electrochemical Characteristics of LiNi1/3Mn1/3Co1/3O2 Electrode with Different Calendering Conditions. *Electrochim. Acta* **2017**, *232*, 431–438. [CrossRef]
53. Schmidt, D.; Kamlah, M.; Knoblauch, V. Highly Densified NCM-Cathodes for High Energy Li-Ion Batteries: Microstructural Evolution during Densification and Its Influence on the Performance of the Electrodes. *J. Energy Storage* **2018**, *17*, 213–223. [CrossRef]
54. Santhanagopalan, S.; White, R.E. Quantifying Cell-to-Cell Variations in Lithium Ion Batteries. *Int. J. Electrochem.* **2012**, *2012*, e395838. [CrossRef]
55. Shin, D.; Poncino, M.; Macii, E.; Chang, N. A Statistical Model-Based Cell-to-Cell Variability Management of Li-Ion Battery Pack. *IEEE Trans. Comput. Aided Des. Integr. Circuits Syst.* **2015**, *34*, 252–265. [CrossRef]
56. Rucci, A.; Ngandjong, A.C.; Primo, E.N.; Maiza, M.; Franco, A.A. Tracking Variabilities in the Simulation of Lithium Ion Battery Electrode Fabrication and Its Impact on Electrochemical Performance. *Electrochim. Acta* **2019**, *312*, 168–178. [CrossRef]
57. Duquesnoy, M.; Lombardo, T.; Chouchane, M.; Primo, E.N.; Franco, A.A. Data-Driven Assessment of Electrode Calendering Process by Combining Experimental Results, in Silico Mesostructures Generation and Machine Learning. *J. Power Sources* **2020**, *480*, 229103. [CrossRef]
58. Leithoff, R.; Fröhlich, A.; Dröder, K. Investigation of the Influence of Deposition Accuracy of Electrodes on the Electrochemical Properties of Lithium-Ion Batteries. *Energy Technol.* **2020**, *8*, 1900129. [CrossRef]
59. Paxton, W.A.; Zhong, Z.; Tsakalakos, T. Tracking Inhomogeneity in High-Capacity Lithium Iron Phosphate Batteries. *J. Power Sources* **2015**, *275*, 429–434. [CrossRef]
60. Ziesche, R.F.; Arlt, T.; Finegan, D.P.; Heenan, T.M.M.; Tengattini, A.; Baum, D.; Kardjilov, N.; Markötter, H.; Manke, I.; Kockelmann, W.; et al. 4D Imaging of Lithium-Batteries Using Correlative Neutron and X-Ray Tomography with a Virtual Unrolling Technique. *Nat. Commun.* **2020**, *11*, 777. [CrossRef]
61. Baumhöfer, T.; Brühl, M.; Rothgang, S.; Sauer, D.U. Production Caused Variation in Capacity Aging Trend and Correlation to Initial Cell Performance. *J. Power Sources* **2014**, *247*, 332–338. [CrossRef]
62. Miyatake, S.; Susuki, Y.; Hikihara, T.; Itoh, S.; Tanaka, K. Discharge Characteristics of Multicell Lithium-Ion Battery with Nonuniform Cells. *J. Power Sources* **2013**, *241*, 736–743. [CrossRef]
63. Gogoana, R.; Pinson, M.B.; Bazant, M.Z.; Sarma, S.E. Internal Resistance Matching for Parallel-Connected Lithium-Ion Cells and Impacts on Battery Pack Cycle Life. *J. Power Sources* **2014**, *252*, 8–13. [CrossRef]
64. Dubarry, M.; Truchot, C.; Cugnet, M.; Liaw, B.Y.; Gering, K.; Sazhin, S.; Jamison, D.; Michelbacher, C. Evaluation of Commercial Lithium-Ion Cells Based on Composite Positive Electrode for Plug-in Hybrid Electric Vehicle Applications. Part I: Initial Characterizations. *J. Power Sources* **2011**, *196*, 10328–10335. [CrossRef]
65. Paul, S.; Diegelmann, C.; Kabza, H.; Tillmetz, W. Analysis of Ageing Inhomogeneities in Lithium-Ion Battery Systems. *J. Power Sources* **2013**, *239*, 642–650. [CrossRef]
66. Rumpf, K.; Naumann, M.; Jossen, A. Experimental Investigation of Parametric Cell-to-Cell Variation and Correlation Based on 1100 Commercial Lithium-Ion Cells. *J. Energy Storage* **2017**, *14*, 224–243. [CrossRef]
67. An, F.; Chen, L.; Huang, J.; Zhang, J.; Li, P. Rate Dependence of Cell-to-Cell Variations of Lithium-Ion Cells. *Sci. Rep.* **2016**, *6*, 35051. [CrossRef]
68. Schuster, S.F.; Brand, M.J.; Berg, P.; Gleissenberger, M.; Jossen, A. Lithium-Ion Cell-to-Cell Variation during Battery Electric Vehicle Operation. *J. Power Sources* **2015**, *297*, 242–251. [CrossRef]
69. Dubarry, M.; Vuillaume, N.; Liaw, B.Y. Origins and Accommodation of Cell Variations in Li-Ion Battery Pack Modeling. *Int. J. Energy Res.* **2010**, *34*, 216–231. [CrossRef]
70. Devie, A.; Dubarry, M. Durability and Reliability of Electric Vehicle Batteries under Electric Utility Grid Operations. Part 1: Cell-to-Cell Variations and Preliminary Testing. *Batteries* **2016**, *2*, 28. [CrossRef]
71. Xie, L.; Ren, D.; Wang, L.; Chen, Z.; Tian, G.; Amine, K.; He, X. A Facile Approach to High Precision Detection of Cell-to-Cell Variation for Li-Ion Batteries. *Sci. Rep.* **2020**, *10*, 7182. [CrossRef]
72. Carter, R.; Klein, E.J.; Atkinson, R.W.; Love, C.T. Mechanical Collapse as Primary Degradation Mode in Mandrel-Free 18650 Li-Ion Cells Operated at 0 °C. *J. Power Sources* **2019**, *437*, 226820. [CrossRef]
73. Pfrang, A.; Kersys, A.; Kriston, A.; Sauer, D.U.; Rahe, C.; Käbitz, S.; Figgemeier, E. Long-Term Cycling Induced Jelly Roll Deformation in Commercial 18650 Cells. *J. Power Sources* **2018**, *392*, 168–175. [CrossRef]
74. Willenberg, L.K.; Dechent, P.; Fuchs, G.; Teuber, M.; Eckert, M.; Graff, M.; Kürten, N.; Sauer, D.U.; Figgemeier, E. The Development of Jelly Roll Deformation in 18650 Lithium-Ion Batteries at Low State of Charge. *J. Electrochem. Soc.* **2020**. [CrossRef]
75. Cannarella, J.; Arnold, C.B. The Effects of Defects on Localized Plating in Lithium-Ion Batteries. *J. Electrochem. Soc.* **2015**, *162*, A1365. [CrossRef]

76. Cannarella, J.; Arnold, C.B. Ion Transport Restriction in Mechanically Strained Separator Membranes. *J. Power Sources* **2013**, *226*, 149–155. [CrossRef]

77. Mühlbauer, M.J.; Petz, D.; Baran, V.; Dolotko, O.; Hofmann, M.; Kostecki, R.; Senyshyn, A. Inhomogeneous Distribution of Lithium and Electrolyte in Aged Li-Ion Cylindrical Cells. *J. Power Sources* **2020**, *475*, 228690. [CrossRef]

78. Petz, D.; Mühlbauer, M.J.; Schökel, A.; Achterhold, K.; Pfeiffer, F.; Pirling, T.; Hofmann, M.; Senyshyn, A. Heterogeneity of Graphite Lithiation in State-of-the-Art Cylinder-Type Li-Ion Cells. *Batter. Supercaps* **2021**, *4*, 327–335. [CrossRef]

79. Mühlbauer, M.J.; Dolotko, O.; Hofmann, M.; Ehrenberg, H.; Senyshyn, A. Effect of Fatigue/Ageing on the Lithium Distribution in Cylinder-Type Li-Ion Batteries. *J. Power Sources* **2017**, *348*, 145–149. [CrossRef]

80. [Infographic] Galaxy Note7: What We Discovered. Available online: https://news.samsung.com/global/infographic-galaxy-note7-what-we-discovered (accessed on 25 February 2021).

81. Loveridge, M.J.; Remy, G.; Kourra, N.; Genieser, R.; Barai, A.; Lain, M.J.; Guo, Y.; Amor-Segan, M.; Williams, M.A.; Amietszajew, T.; et al. Looking Deeper into the Galaxy (Note 7). *Batteries* **2018**, *4*, 3. [CrossRef]

82. Werner, D.; Paarmann, S.; Wiebelt, A.; Wetzel, T. Inhomogeneous Temperature Distribution Affecting the Cyclic Aging of Li-Ion Cells. Part II: Analysis and Correlation. *Batteries* **2020**, *6*, 12. [CrossRef]

83. Osswald, P.J.; Erhard, S.V.; Rheinfeld, A.; Rieger, B.; Hoster, H.E.; Jossen, A. Temperature Dependency of State of Charge Inhomogeneities and Their Equalization in Cylindrical Lithium-Ion Cells. *J. Power Sources* **2016**, *329*, 546–552. [CrossRef]

84. Grandjean, T.; Barai, A.; Hosseinzadeh, E.; Guo, Y.; McGordon, A.; Marco, J. Large Format Lithium Ion Pouch Cell Full Thermal Characterisation for Improved Electric Vehicle Thermal Management. *J. Power Sources* **2017**, *359*, 215–225. [CrossRef]

85. Carter, R.; Kingston, T.A.; Atkinson, R.W.; Parmananda, M.; Dubarry, M.; Fear, C.; Mukherjee, P.P.; Love, C.T. Directionality of Thermal Gradients in Lithium-Ion Batteries Dictates Diverging Degradation Modes. *Cell Rep. Phys. Sci.* **2021**, 100351. [CrossRef]

86. Paarmann, S.; Cloos, L.; Technau, J.; Wetzel, T. Measurement of the Temperature Influence on the Current Distribution in Li-Ion Batteries. *Energy Technol.* **2020**, ente.202000862. [CrossRef]

87. Moretti, A.; Carvalho, D.V.; Ehteshami, N.; Paillard, E.; Porcher, W.; Brun-Buisson, D.; Ducros, J.-B.; de Meatza, I.; Eguia-Barrio, A.; Trad, K.; et al. A Post-Mortem Study of Stacked 16 Ah Graphite//LiFePO4 Pouch Cells Cycled at 5 °C. *Batteries* **2019**, *5*, 45. [CrossRef]

88. Robinson, J.B.; Maier, M.; Alster, G.; Compton, T.; Brett, D.J.L.; Shearing, P.R. Spatially Resolved Ultrasound Diagnostics of Li-Ion Battery Electrodes. *Phys. Chem. Chem. Phys.* **2019**, *21*, 6354–6361. [CrossRef]

89. Rowden, B.; Garcia-Araez, N. A Review of Gas Evolution in Lithium Ion Batteries. *Energy Rep.* **2020**, *6*, 10–18. [CrossRef]

90. Michalowski, P.; Gräfenstein, A.; Knipper, M.; Plaggenborg, T.; Schwenzel, J.; Parisi, J. Examining Inhomogeneous Degradation of Graphite/Carbon Black Composite Electrodes in Li-Ion Batteries by Lock-In Thermography. *J. Electrochem. Soc.* **2017**, *164*, A2251. [CrossRef]

91. Devie, A.; Dubarry, M.; Liaw, B.Y. Overcharge Study in Li4Ti5O12 Based Lithium-Ion Pouch Cell: I. Quantitative Diagnosis of Degradation Modes. *J. Electrochem. Soc.* **2015**, *162*, A1033. [CrossRef]

92. Devie, A.; Dubarry, M.; Wu, H.-P.; Wu, T.-H.; Liaw, B.Y. Overcharge Study in Li4Ti5O12 Based Lithium-Ion Pouch Cell. *J. Electrochem. Soc.* **2016**, *163*, A2611. [CrossRef]

93. Devie, A.; Baure, G.; Dubarry, M. Intrinsic Variability in the Degradation of a Batch of Commercial 18650 Lithium-Ion Cells. *Energies* **2018**, *11*, 1031. [CrossRef]

94. Harris, S.J.; Harris, D.J.; Li, C. Failure Statistics for Commercial Lithium Ion Batteries: A Study of 24 Pouch Cells. *J. Power Sources* **2017**, *342*, 589–597. [CrossRef]

95. Li, W.; Sengupta, N.; Dechent, P.; Howey, D.; Annaswamy, A.; Sauer, D.U. Online Capacity Estimation of Lithium-Ion Batteries with Deep Long Short-Term Memory Networks. *J. Power Sources* **2021**, *482*, 228863. [CrossRef]

96. Pastor-Fernández, C.; Bruen, T.; Widanage, W.D.; Gama-Valdez, M.A.; Marco, J. A Study of Cell-to-Cell Interactions and Degradation in Parallel Strings: Implications for the Battery Management System. *J. Power Sources* **2016**, *329*, 574–585. [CrossRef]

97. Brand, M.J.; Schmidt, P.A.; Zaeh, M.F.; Jossen, A. Welding Techniques for Battery Cells and Resulting Electrical Contact Resistances. *J. Energy Storage* **2015**, *1*, 7–14. [CrossRef]

98. Taylor, J.; Barai, A.; Ashwin, T.R.; Guo, Y.; Amor-Segan, M.; Marco, J. An Insight into the Errors and Uncertainty of the Lithium-Ion Battery Characterisation Experiments. *J. Energy Storage* **2019**, *24*, 100761. [CrossRef]

99. Bruen, T.; Marco, J. Modelling and Experimental Evaluation of Parallel Connected Lithium Ion Cells for an Electric Vehicle Battery System. *J. Power Sources* **2016**, *310*, 91–101. [CrossRef]

100. Wang, L.; Cheng, Y.; Zhao, X. Influence of Connecting Plate Resistance upon LiFePO4 Battery Performance. *Appl. Energy* **2015**, *147*, 353–360. [CrossRef]

101. Offer, G.J.; Yufit, V.; Howey, D.A.; Wu, B.; Brandon, N.P. Module Design and Fault Diagnosis in Electric Vehicle Batteries. *J. Power Sources* **2012**, *206*, 383–392. [CrossRef]

102. Naguib, M.; Kollmeyer, P.; Emadi, A. Lithium-Ion Battery Pack Robust State of Charge Estimation, Cell Inconsistency, and Balancing: Review. *IEEE Access* **2021**, *9*, 50570–50582. [CrossRef]

103. Dubarry, M.; Vuillaume, N.; Liaw, B.Y. From Single Cell Model to Battery Pack Simulation for Li-Ion Batteries. *J. Power Sources* **2009**, *186*, 500–507. [CrossRef]

104. Dubarry, M.; Pastor-Fernández, C.; Baure, G.; Yu, T.F.; Widanage, W.D.; Marco, J. Battery Energy Storage System Modeling: Investigation of Intrinsic Cell-to-Cell Variations. *J. Energy Storage* **2019**, *23*, 19–28. [CrossRef]

105. Feng, F.; Hu, X.; Hu, L.; Hu, F.; Li, Y.; Zhang, L. Propagation Mechanisms and Diagnosis of Parameter Inconsistency within Li-Ion Battery Packs. *Renew. Sustain. Energy Rev.* **2019**, *112*, 102–113. [CrossRef]
106. Liu, X.; Ai, W.; Naylor Marlow, M.; Patel, Y.; Wu, B. The Effect of Cell-to-Cell Variations and Thermal Gradients on the Performance and Degradation of Lithium-Ion Battery Packs. *Appl. Energy* **2019**, *248*, 489–499. [CrossRef]
107. Neupert, S.; Kowal, J. Inhomogeneities in Battery Packs. *World Electr. Veh. J.* **2018**, *9*, 20. [CrossRef]
108. Wu, B.; Yufit, V.; Marinescu, M.; Offer, G.J.; Martinez-Botas, R.F.; Brandon, N.P. Coupled Thermal–Electrochemical Modelling of Uneven Heat Generation in Lithium-Ion Battery Packs. *J. Power Sources* **2013**, *243*, 544–554. [CrossRef]
109. Dubarry, M.; Devie, A.; Stein, K.; Tun, M.; Matsuura, M.; Rocheleau, R. Battery Energy Storage System Battery Durability and Reliability under Electric Utility Grid Operations: Analysis of 3 Years of Real Usage. *J. Power Sources* **2017**, *338*, 65–73. [CrossRef]
110. Yang, N.; Zhang, X.; Shang, B.; Li, G. Unbalanced Discharging and Aging Due to Temperature Differences among the Cells in a Lithium-Ion Battery Pack with Parallel Combination. *J. Power Sources* **2016**, *306*, 733–741. [CrossRef]
111. Chiu, K.-C.; Lin, C.-H.; Yeh, S.-F.; Lin, Y.-H.; Huang, C.-S.; Chen, K.-C. Cycle Life Analysis of Series Connected Lithium-Ion Batteries with Temperature Difference. *J. Power Sources* **2014**, *263*, 75–84. [CrossRef]
112. An, F.; Huang, J.; Wang, C.; Li, Z.; Zhang, J.; Wang, S.; Li, P. Cell Sorting for Parallel Lithium-Ion Battery Systems: Evaluation Based on an Electric Circuit Model. *J. Energy Storage* **2016**, *6*, 195–203. [CrossRef]
113. Lyu, C.; Song, Y.; Wang, L.; Li, J.; Zhang, B.; Liu, E. A New Method for Lithium-Ion Battery Uniformity Sorting Based on Internal Criteria. *J. Energy Storage* **2019**, *25*, 100885. [CrossRef]
114. Wang, T.; Tseng, K.J.; Zhao, J.; Wei, Z. Thermal Investigation of Lithium-Ion Battery Module with Different Cell Arrangement Structures and Forced Air-Cooling Strategies. *Appl. Energy* **2014**, *134*, 229–238. [CrossRef]
115. Gering, K.L.; Sazhin, S.V.; Jamison, D.K.; Michelbacher, C.J.; Liaw, B.Y.; Dubarry, M.; Cugnet, M. Investigation of Path Dependence in Commercial Lithium-Ion Cells Chosen for Plug-in Hybrid Vehicle Duty Cycle Protocols. *J. Power Sources* **2011**, *196*, 3395–3403. [CrossRef]
116. Keil, J.; Paul, N.; Baran, V.; Keil, P.; Gilles, R.; Jossen, A. Linear and Nonlinear Aging of Lithium-Ion Cells Investigated by Electrochemical Analysis and In-Situ Neutron Diffraction. *J. Electrochem. Soc.* **2019**, *166*, A3908. [CrossRef]
117. Raj, T.; Wang, A.A.; Monroe, C.W.; Howey, D.A. Investigation of Path-Dependent Degradation in Lithium-Ion Batteries**. *Batter. Supercaps* **2020**, *3*, 1377–1385. [CrossRef]
118. Simolka, M.; Heger, J.-F.; Kaess, H.; Biswas, I.; Friedrich, K.A. Influence of Cycling Profile, Depth of Discharge and Temperature on Commercial LFP/C Cell Ageing: Post-Mortem Material Analysis of Structure, Morphology and Chemical Composition. *J. Appl. Electrochem.* **2020**, *50*, 1101–1117. [CrossRef]
119. Anseán, D.; Dubarry, M.; Devie, A.; Liaw, B.Y.; García, V.M.; Viera, J.C.; González, M. Operando Lithium Plating Quantification and Early Detection of a Commercial LiFePO4 Cell Cycled under Dynamic Driving Schedule. *J. Power Sources* **2017**, *356*, 36–46. [CrossRef]
120. Liaw, B.Y.; Dubarry, M. From Driving Cycle Analysis to Understanding Battery Performance in Real-Life Electric Hybrid Vehicle Operation. *J. Power Sources* **2007**, *174*, 76–88. [CrossRef]
121. Martinez-Laserna, E.; Sarasketa-Zabala, E.; Stroe, D.-I.; Swierczynski, M.; Warnecke, A.; Timmermans, J.M.; Goutam, S.; Rodriguez, P. Evaluation of Lithium-Ion Battery Second Life Performance and Degradation. In Proceedings of the 2016 IEEE Energy Conversion Congress and Exposition (ECCE), Milwaukee, WI, USA, 18–22 September 2016; pp. 1–7.
122. Hossain, E.; Murtaugh, D.; Mody, J.; Faruque, H.M.R.; Sunny, M.S.H.; Mohammad, N. A Comprehensive Review on Second-Life Batteries: Current State, Manufacturing Considerations, Applications, Impacts, Barriers Potential Solutions, Business Strategies, and Policies. *IEEE Access* **2019**, *7*, 73215–73252. [CrossRef]
123. Glazer, M.P.B.; Okasinski, J.S.; Almer, J.D.; Ren, Y. High-Energy X-ray Scattering Studies of Battery Materials. *MRS Bull.* **2016**, *41*, 460–465. [CrossRef]
124. Müller, S.; Pietsch, P.; Brandt, B.-E.; Baade, P.; Andrade, V.D.; Carlo, F.D.; Wood, V. Quantification and Modeling of Mechanical Degradation in Lithium-Ion Batteries Based on Nanoscale Imaging. *Nat. Commun.* **2018**, *9*, 2340. [CrossRef] [PubMed]
125. Cai, L.; An, K.; Feng, Z.; Liang, C.; Harris, S.J. In-Situ Observation of Inhomogeneous Degradation in Large Format Li-Ion Cells by Neutron Diffraction. *J. Power Sources* **2013**, *236*, 163–168. [CrossRef]
126. Senyshyn, A.; Mühlbauer, M.J.; Dolotko, O.; Hofmann, M.; Ehrenberg, H. Homogeneity of Lithium Distribution in Cylinder-Type Li-Ion Batteries. *Sci. Rep.* **2015**, *5*, 18380. [CrossRef]
127. Paul, N.; Wandt, J.; Seidlmayer, S.; Schebesta, S.; Mühlbauer, M.J.; Dolotko, O.; Gasteiger, H.A.; Gilles, R. Aging Behavior of Lithium Iron Phosphate Based 18650-Type Cells Studied by in Situ Neutron Diffraction. *J. Power Sources* **2017**, *345*, 85–96. [CrossRef]
128. Paul, N.; Keil, J.; Kindermann, F.M.; Schebesta, S.; Dolotko, O.; Mühlbauer, M.J.; Kraft, L.; Erhard, S.V.; Jossen, A.; Gilles, R. Aging in 18650-Type Li-Ion Cells Examined with Neutron Diffraction, Electrochemical Analysis and Physico-Chemical Modeling. *J. Energy Storage* **2018**, *17*, 383–394. [CrossRef]
129. Zinth, V.; von Lüders, C.; Wilhelm, J.; Erhard, S.V.; Hofmann, M.; Seidlmayer, S.; Rebelo-Kornmeier, J.; Gan, W.; Jossen, A.; Gilles, R. Inhomogeneity and Relaxation Phenomena in the Graphite Anode of a Lithium-Ion Battery Probed by in Situ Neutron Diffraction. *J. Power Sources* **2017**, *361*, 54–60. [CrossRef]
130. Petz, D.; Mühlbauer, M.J.; Baran, V.; Frost, M.; Schökel, A.; Paulmann, C.; Chen, Y.; Garcés, D.; Senyshyn, A. Lithium Heterogeneities in Cylinder-Type Li-Ion Batteries—Fatigue Induced by Cycling. *J. Power Sources* **2020**, *448*, 227466. [CrossRef]

131. Fleming, J.; Amietszajew, T.; Charmet, J.; Roberts, A.J.; Greenwood, D.; Bhagat, R. The Design and Impact of In-Situ and Operando Thermal Sensing for Smart Energy Storage. *J. Energy Storage* **2019**, *22*, 36–43. [CrossRef]

132. McTurk, E.; Birkl, C.R.; Roberts, M.R.; Howey, D.A.; Bruce, P.G. Minimally Invasive Insertion of Reference Electrodes into Commercial Lithium-Ion Pouch Cells. *ECS Electrochem. Lett.* **2015**, *4*, A145. [CrossRef]

133. Osswald, P.J.; Erhard, S.V.; Noel, A.; Keil, P.; Kindermann, F.M.; Hoster, H.; Jossen, A. Current Density Distribution in Cylindrical Li-Ion Cells during Impedance Measurements. *J. Power Sources* **2016**, *314*, 93–101. [CrossRef]

134. Wang, H.; Whitacre, J.F. Inhomogeneous Aging of Cathode Materials in Commercial 18650 Lithium Ion Battery Cells. *J. Energy Storage* **2021**, *35*, 102244. [CrossRef]

135. Warnecke, A.J. Degradation Mechanisms in NMC-Based Lithium-Ion Batteries. Ph.D. Thesis, RWTH Aachen University, Aachen, Germany, 2017.

136. Gyenes, B.; Stevens, D.A.; Chevrier, V.L.; Dahn, J.R. Understanding Anomalous Behavior in Coulombic Efficiency Measurements on Li-Ion Batteries. *J. Electrochem. Soc.* **2015**, *162*, A278–A283. [CrossRef]

137. Juarez-Robles, D.; Jeevarajan, J.A.; Mukherjee, P.P. Degradation-Safety Analytics in Lithium-Ion Cells: Part I. Aging under Charge/Discharge Cycling. *J. Electrochem. Soc.* **2020**, *167*, 160510. [CrossRef]

138. Spingler, F.B.; Naumann, M.; Jossen, A. Capacity Recovery Effect in Commercial LiFePO4 / Graphite Cells. *J. Electrochem. Soc.* **2020**, *167*, 040526. [CrossRef]

139. Burns, J.C.; Stevens, D.A.; Dahn, J.R. In-Situ Detection of Lithium Plating Using High Precision Coulometry. *J. Electrochem. Soc.* **2015**, *162*, A959–A964. [CrossRef]

140. Lewerenz, M.; Warnecke, A.; Sauer, D.U. Post-Mortem Analysis on LiFePO4|Graphite Cells Describing the Evolution & Composition of Covering Layer on Anode and Their Impact on Cell Performance. *J. Power Sources* **2017**, *369*, 122–132. [CrossRef]

141. Fleury, X.; Noh, M.H.; Geniès, S.; Thivel, P.X.; Lefrou, C.; Bultel, Y. Fast-Charging of Lithium Iron Phosphate Battery with Ohmic-Drop Compensation Method: Ageing Study. *J. Energy Storage* **2018**, *16*, 21–36. [CrossRef]

142. Käbitz, S. Untersuchung der Alterung von Lithium-Ionen-Batterien Mittels Elektroanalytik und Elektrochemischer Impedanzspektroskopie. Ph.D. Thesis, RWTH Aachen University, Aachen, Germany, 2016.

143. Pfrang, A.; Kersys, A.; Kriston, A.; Sauer, D.U.; Rahe, C.; Käbitz, S.; Figgemeier, E. Geometrical Inhomogeneities as Cause of Mechanical Failure in Commercial 18650 Lithium Ion Cells. *J. Electrochem. Soc.* **2019**, *166*, A3745–A3752. [CrossRef]

144. Burow, D.; Sergeeva, K.; Calles, S.; Schorb, K.; Börger, A.; Roth, C.; Heitjans, P. Inhomogeneous Degradation of Graphite Anodes in Automotive Lithium Ion Batteries under Low-Temperature Pulse Cycling Conditions. *J. Power Sources* **2016**, *307*, 806–814. [CrossRef]

145. Rahe, C.; Kelly, S.T.; Rad, M.N.; Sauer, D.U.; Mayer, J.; Figgemeier, E. Nanoscale X-Ray Imaging of Ageing in Automotive Lithium Ion Battery Cells. *J. Power Sources* **2019**, *433*, 126631. [CrossRef]

146. Yang, Y.; Xu, R.; Zhang, K.; Lee, S.-J.; Mu, L.; Liu, P.; Waters, C.K.; Spence, S.; Xu, Z.; Wei, C.; et al. Quantification of Heterogeneous Degradation in Li-Ion Batteries. *Adv. Energy Mater.* **2019**, *9*, 1900674. [CrossRef]

147. Li, L.; Hou, J. Capacity Detection of Electric Vehicle Lithium-Ion Batteries Based on X-Ray Computed Tomography. *RSC Adv.* **2018**, *8*, 25325–25333. [CrossRef]

148. Ilott, A.J.; Mohammadi, M.; Schauerman, C.M.; Ganter, M.J.; Jerschow, A. Rechargeable Lithium-Ion Cell State of Charge and Defect Detection by in-Situ inside-out Magnetic Resonance Imaging. *Nat. Commun.* **2018**, *9*, 1776. [CrossRef]

149. Krachkovskiy, S.A.; Foster, J.M.; Bazak, J.D.; Balcom, B.J.; Goward, G.R. Operando Mapping of Li Concentration Profiles and Phase Transformations in Graphite Electrodes by Magnetic Resonance Imaging and Nuclear Magnetic Resonance Spectroscopy. *J. Phys. Chem. C* **2018**, *122*, 21784–21791. [CrossRef]

150. Wiemers-Meyer, S.; Winter, M.; Nowak, S. Mechanistic Insights into Lithium Ion Battery Electrolyte Degradation—A Quantitative NMR Study. *Phys. Chem. Chem. Phys.* **2016**, *18*, 26595–26601. [CrossRef] [PubMed]

151. Bauermann, L.P.; Mesquita, L.V.; Bischoff, C.; Drews, M.; Fitz, O.; Heuer, A.; Biro, D. Scanning Acoustic Microscopy as a Non-Destructive Imaging Tool to Localize Defects inside Battery Cells. *J. Power Sources Adv.* **2020**, *6*, 100035. [CrossRef]

152. Dubarry, M.; Baure, G. Perspective on Commercial Li-Ion Battery Testing, Best Practices for Simple and Effective Protocols. *Electronics* **2020**, *9*, 152. [CrossRef]

153. Meddings, N.; Heinrich, M.; Overney, F.; Lee, J.-S.; Ruiz, V.; Napolitano, E.; Seitz, S.; Hinds, G.; Raccichini, R.; Gaberšček, M.; et al. Application of Electrochemical Impedance Spectroscopy to Commercial Li-Ion Cells: A Review. *J. Power Sources* **2020**, *480*, 228742. [CrossRef]

154. Bloom, I.; Jansen, A.N.; Abraham, D.P.; Knuth, J.; Jones, S.A.; Battaglia, V.S.; Henriksen, G.L. Differential Voltage Analyses of High-Power, Lithium-Ion Cells 1. Technique and Application. *J. Power Sources* **2005**, *139*, 295–303. [CrossRef]

155. Dubarry, M.; Liaw, B.Y. Identify Capacity Fading Mechanism in a Commercial LiFePO4 Cell. *J. Power Sources* **2009**, *194*, 541–549. [CrossRef]

156. Lewerenz, M.; Marongiu, A.; Warnecke, A.; Sauer, D.U. Differential Voltage Analysis as a Tool for Analyzing Inhomogeneous Aging: A Case Study for LiFePO4|Graphite Cylindrical Cells. *J. Power Sources* **2017**, *368*, 57–67. [CrossRef]

157. Jiang, Y.; Jiang, J.; Zhang, C.; Zhang, W.; Gao, Y.; Guo, Q. Recognition of Battery Aging Variations for LiFePO4 Batteries in 2nd Use Applications Combining Incremental Capacity Analysis and Statistical Approaches. *J. Power Sources* **2017**, *360*, 180–188. [CrossRef]

158. Tanim, T.R.; Shirk, M.G.; Bewley, R.L.; Dufek, E.J.; Liaw, B.Y. Fast Charge Implications: Pack and Cell Analysis and Comparison. *J. Power Sources* **2018**, *381*, 56–65. [CrossRef]

159. Chang, L.; Wang, C.; Zhang, C.; Xiao, L.; Cui, N.; Li, H.; Qiu, J. A Novel Fast Capacity Estimation Method Based on Current Curves of Parallel-Connected Cells for Retired Lithium-Ion Batteries in Second-Use Applications. *J. Power Sources* **2020**, *459*, 227901. [CrossRef]

160. Krupp, A.; Ferg, E.; Schuldt, F.; Derendorf, K.; Agert, C. Incremental Capacity Analysis as a State of Health Estimation Method for Lithium-Ion Battery Modules with Series-Connected Cells. *Batteries* **2021**, *7*, 2. [CrossRef]

161. Lewerenz, M.; Warnecke, A.; Sauer, D.U. Introduction of Capacity Difference Analysis (CDA) for Analyzing Lateral Lithium-Ion Flow to Determine the State of Covering Layer Evolution. *J. Power Sources* **2017**, *354*, 157–166. [CrossRef]

162. Prosser, R.; Offer, G.; Patel, Y. Lithium-Ion Diagnostics: The First Quantitative In-Operando Technique for Diagnosing Lithium Ion Battery Degradation Modes under Load with Realistic Thermal Boundary Conditions. *J. Electrochem. Soc.* **2021**, *168*, 030532. [CrossRef]

163. Delobel, B. Lessons Learned from Field Data Analysis, and Future Challenges—Renault EV 2019. Available online: http://cii-resource.com/cet/AABE-03-17/Presentations/BMGT/Delobel_Bruno.pdf (accessed on 1 June 2021).

164. Salinas, F.; Krüger, L.; Neupert, S.; Kowal, J. A Second Life for Li-Ion Cells Rescued from Notebook Batteries. *J. Energy Storage* **2019**, *24*, 100747. [CrossRef]

165. Myall, D. 30 KWh Nissan Leaf Firmware Update to Correct Capacity Reporting. *FlipTheFleet* **2018**. Available online: https://flipthefleet.org/2018/30-kwh-nissan-leaf-firmware-update-to-correct-capacity-reporting/ (accessed on 1 June 2021).

166. MaxRange Tesla Battery Survey. Available online: https://teslamotorsclub.com/tmc/threads/maxrange.35978/ (accessed on 7 March 2021).